Worsley, S. F., T. M. Innocent, N. A. Holmes, M. M. Al-Bassam, M. Schiøtt, B. Wilkinson, J. C. Murrell, J. J. Boomsma, D. W. Yu, and M. I. Hutchings. 2021. Competition-based screening helps to secure the evolutionary stability of a defensive microbiome. BMC Biology 19:205.

Competition-based screening helps to secure the evolutionary stability of a defensive microbiome

Sarah F. Worsley[1], Tabitha M. Innocent[2,†], Neil A. Holmes[1,3,†], Mahmoud M. Al-Bassam[1], Morten Schiøtt[2], Barrie Wilkinson[3], J. Colin Murrell[4], Jacobus J. Boomsma[2*], Douglas W. Yu[1,5,6,*], Matthew I. Hutchings[1,3,*]

[1]School of Biological Sciences, University of East Anglia, Norwich Research Park, Norwich, Norfolk, UK NR47TJ

[2]Centre for Social Evolution, Section for Ecology and Evolution, Department of Biology, University of Copenhagen, Copenhagen, Denmark.

[3]Department of Molecular Microbiology, John Innes Centre, Norwich Research Park, Norwich, Norfolk, UK NR47UH

[4]School of Environmental Sciences, University of East Anglia, Norwich Research Park, Norwich, Norfolk, UK NR47TJ

[5]State Key Laboratory of Genetic Resources and Evolution, Kunming Institute of Zoology, Chinese Academy of Sciences, Kunming, Yunnan, China 650223

[6]Center for Excellence in Animal Evolution and Genetics, Chinese Academy of Sciences, Kunming Yunnan, China 650223

†These authors contributed equally to the manuscript

*Correspondence: matt.hutchings@jic.ac.uk, jjboomsma@bio.ku.dk, douglas.yu@uea.ac.uk

Abstract

Background

The cuticular microbiomes of *Acromyrmex* leaf-cutting ants pose a conundrum in microbiome biology because they are freely colonizable, and yet the prevalence of the vertically transmitted bacteria *Pseudonocardia*, which contributes to the control of *Escovopsis* fungus-garden disease, is never compromised by the secondary acquisition of other bacterial strains. Game theory suggests that *competition-based screening* can allow the selective recruitment of antibiotic-producing bacteria from the environment, by providing abundant resources to foment interference competition between bacterial species, and by using *Pseudonocardia* to bias the outcome of competition in favour of antibiotic producers.

Results

Here we use RNA-stable isotope probing (RNA-SIP) to confirm that *Acromyrmex* ants can maintain a range of microbial symbionts on their cuticle by supplying public resources. We then used RNA-sequencing, bioassays, and competition experiments to show that vertically transmitted *Pseudonocardia* strains produce antibacterials that differentially reduce the growth rates of other microbes, ultimately biasing bacterial competition to allow the selective establishment of secondary antibiotic-producing strains while excluding non-antibiotic-producing strains that would parasitize the symbiosis.

Conclusions

Our findings are consistent with the hypothesis that competition-based screening is a plausible mechanism for maintaining the integrity of the co-adapted mutualism between the leaf-cutting ant farming symbiosis and its defensive microbiome. Our results have broader implications for explaining the stability of other complex symbioses involving horizontal acquisition.

Keywords: antibiotics, Attini, game theory, defensive microbiome, mutualism, Actinobacteria, partner, leaf-cutting ants, *Pseudonocardia*, interference competition, horizontal acquisition, symbiosis

Background

The diversity of insect associated microbial communities is staggering. They may consist of single intracellular symbionts with reduced genomes owing to coadaptation at one extreme [1], to dynamic microbiomes in open host compartments such as guts at the other end of the scale [2]. Insect microbiomes have been intensively studied across a range of species, and there is increasing consensus regarding their vital contributions to host fitness throughout ontogenetic development [3-6]. However, the stability and cooperative characteristics of complex microbiomes is a paradox. While relentless competition is the default setting of the microbial world [7], hosts appear to evolve control by holding their microbiome ecosystems on a leash [8], but how dynamic stability under continuing turnover is achieved remains unclear. Despite an abundance of microbiome research, recent reviews have concluded that "integration between theory and experiments is a crucial 'missing link' in current microbial ecology" [9] and that "our ability to make predictions about these dynamic, highly complex communities is limited" [10].

Game theory suggests a compelling solution to the unity-in-diversity paradox by showing that *competition-based screening* can be a powerful mechanism to maintain cooperative stability. Screening is likely to work when hosts evolve (1) to provide nutrients and/or space to foment competition amongst symbionts, thus creating an attractive but 'demanding' environment, and (2) to skew the resulting competition such that mutualistic symbionts enjoy a competitive advantage. Competitive exclusion then 'screens-in' mutualists and 'screens-out' parasitic and free-rider symbionts [11-13]. Screening is conceptually clearest when the symbiont trait that confers competitive superiority is the same as (or strongly correlated with) the trait that benefits the host. An illustration of such correlated functionality was provided by Heil [14] who showed that ant-hosting acacia plants provide copious food bodies, which fuels the production of numerous, actively patrolling ant workers. The ant species whose colony invests in greater numbers of aggressive workers outcompetes other ant colonies trying to establish on the same plant, and the same investment in aggressive workers is likely to better protect the host plants against herbivores [14].

Screening has also been suggested to act in animal-microbe symbioses. For instance, Tragust et al. [15] showed that carpenter ants acidify their own stomachs by swallowing acidopore secretions. Entomopathogenic bacteria are then rapidly killed off, whereas the co-adapted gut bacterial symbiont *Asaia* sp. (Acetobacteraceae) exhibits a lower mortality rate and

maintains itself in the midgut. Addressing a similar question, Itoh *et al*. [16] used co-inoculation experiments to show that environmentally recruited but co-adapted 'native' *Burkholderia* symbionts outcompete non-native bacteria in the gut of their bean bug host, even though they are able to establish in the absence of the 'native' symbiont. Finally, Ranger *et al*. [17] showed that ambrosia beetles selectively colonize physiologically stressed trees, which have a high ethanol titre due to anaerobic respiration. The vertically transmitted fungal symbionts of these beetles have evolved to detoxify the ethanol whereas competing weedy fungi remain inhibited.

Competition-based screening seems particularly apt for the establishment of protective microbiomes [12, 13] because although the production of bioactive compounds such as antibiotics is highly complex, leading to a wide diversity of chemical structures and resistance mechanisms, natural selection is expected to reinforce the correlation between the traits of antibiotic production and antibiotic resistance, since production without resistance by the same cell would be suicidal. Scheuring and Yu [12] thus proposed that if a host species provides copious food resources and if non-producer strains have the faster growth rate, the microbiome becomes 'bistable,' meaning that two equilibrium outcomes are possible. If the non-producers start with a higher initial abundance, their faster growth rate allows them to take over the host space and exclude the antibiotic-producers before the latter can produce high concentrations of antibiotic, whereas if the slower-growing antibiotic producers start with a higher initial abundance, they have a large enough population to produce enough antibiotic to kill off non-producers, and grow to take over the host space. In this light, vertical transmission of an antibiotic producer strain by the host can ensure that the microbiome always starts with a higher abundance of antibiotic producers.

The conservative assumption in this argument is that the non-producers are given the faster growth rate, which is likely, since they do not pay the cost of antibiotic production and since non-producers are more common than producers in the environment, which implies that in any random sample of microbial colonisers from the environment, at least some of the non-producers are likely to have faster growth rates than producers. Under such circumstances, vertical transmission of a primary antibiotic producer can result in the selective horizontal acquisition (recruitment) of additional, antibiotic-producing bacteria from the environment, because antibiotic-producers should be superior competitors in food- and antibiotic-filled environments. The resulting, more diverse, microbiomes are then largely purged of free-riding non-beneficial strains [8, 11, 12]. Previous research has shown that the protective, cuticular

microbiome of *Acromyrmex echinatior* leaf-cutting ants (Formicidae, Attini) is an ideal model system to test whether screening can act as a leash in the ecosystem-on-a-leash perspective [8, 18].

Acromyrmex worker ants forage for fresh leaf fragments to provision their co-evolved fungus-garden mutualist *Leucoagaricus gongylophorus* [19, 20]. The fungal cultivar produces gongylidia, nutrient-rich swellings that are the sole food source for the queen and larvae [21, 22] and the predominant food source for the workers who also ingest plant-sap and fruit juice in addition to fungal food [23]. However, *Leucoagaricus* is at risk of being parasitized by the specialized, coevolved mould *Escovopsis weberi*, which can degrade the fungal cultivar and also cause severe ant paralysis and mortality [24-27]. To prevent infections, leaf-cutting ants have evolved a range of weeding and grooming behaviours [28-30], and *A. echinatior* and other *Acromyrmex* species also maintain filamentous actinomycete bacteria that grow as a white bloom on the cuticles of large workers. These bacteria produce antimicrobials that inhibit the growth of *E. weberi* [24, 26, 31]. In Panama, where almost all fieldwork on this multipartite symbiosis has been carried out, the cuticle of *Acromyrmex* workers is dominated by one of two vertically transmitted strains of *Pseudonocardia*, named *P. octospinosus* (Ps1) and *P. echinatior* (Ps2) [18, 32, 33].

Newly eclosed large workers are inoculated with the vertically transmitted *Pseudonocardia* strain by their nestmates. This blooms over the cuticle, reaching maximum coverage after ca. six weeks, before shrinking back to the propleural plates as the ants mature to assume foraging tasks [34, 35]. However, several studies have also identified other actinomycete strains on the propleural plates of *A. echinatior*, which are presumed to be acquired from the environment [18, 36-40]. This includes species of the bacterial genus *Streptomyces*, which have been identified on ants maintained in laboratory-based colonies [36-38], as well as in a 16S rRNA gene amplicon sequencing study of ants sampled from their native environment, although many of these could also have been close relatives of *Streptomyces* [18]. Species of this actinomycete genus produce a variety of antimicrobials so their additional presence may suggest a form of multi-drug therapy against *Escovopsis* [37-39]. However, these putative functions remain enigmatic because *Streptomyces* symbionts were never found on the callow workers [18] that execute hygienic and defensive fungus-garden tasks [35]. In terms of resources, the propleural plates have a high concentration of tiny subcuticular glands, which are presumed to supply the cuticular microbiome with resources [41]. These plates can thus be conjectured to create the food-rich but antibiotic-laden

demanding environment that competition-based screening assumes, because the vertically transmitted native *Pseudonocardia* symbiont always colonizes the propleural plates first [12, 35]. We have previously shown that both *P. octospinosus* and *P. echinatior* encode and make antibacterial compounds that inhibit multiple unicellular bacteria but do not inhibit *Streptomyces* species [32]. However, the other key elements of the screening hypothesis have remained untested.

The present study carries out a series of tests of competition-based screening, using the cuticular microbiome of *A. echinatior* as an open symbiotic ecosystem where the host nonetheless holds the leash, by controlling resource provisioning rates and by having first inoculated workers with *Pseudonocardia*. The co-adapted defensive *Pseudonocardia* symbiont, which is advantaged due to the priority effects associated with vertical transmission, is then expected to skew subsequent competition amongst an unspecified number of symbionts randomly colonising from the environment. We used RNA-SIP (stable isotope probing) to show that the ants provide a food resource on their cuticles that is consumed by multiple bacterial species, thus showing both that the resource is public, and that multiple bacterial species can become established in the cuticular microbiome. We then use RNA sequencing to show, *in vivo*, that mutualistic *P. octospinosus* and *P. echinatior* strains express antibacterial biosynthetic gene clusters (BGCs) on the ant cuticle. Next, we show that diffusible metabolites of these *Pseudonocardia* species exhibit broad-spectrum antibacterial activity *in vitro*, but only weakly inhibit *Streptomyces* species isolated from the cuticular microbiome, which we separately and directly show are resistant to a range of antibiotics. Finally, we demonstrate that these elements result in biased competition, by using *in-vitro* competition experiments to show that slower-growing *Streptomyces* species can competitively exclude faster-growing non-antibacterial-producing species, but only when grown on media infused with *Pseudonocardia* metabolites.

Results

The host provides public resources to its cuticular microbiome. RNA-SIP tracks the flow of heavy isotopes from the host to the RNA of microbial partners that metabolize host-derived resources [42-44]. Labelled and unlabelled RNA within a sample can be separated via ultracentrifugation and fractionation; these fractions can be used as templates for 16S rRNA gene amplicon sequencing so that the bacterial taxa that do (and do not) use host-supplied

resources can be identified [44]. RNA was chosen over DNA in this experiment to increase the chances of labelling over a short time-frame; RNA labelling requires active transcription, whereas DNA labelling requires DNA replication. Actinomycetes, in particular, only massively upregulate DNA replication when they sporulate. A shorter period was also desirable as it reduces any cross-feeding between bacterial species, although we note that any resources acquired by cross-feeding count as public in the screening model because they also, eventually, contribute to bacterial growth and metabolism. Three replicate groups of 22 mature worker ants were fed a 20% (w/v) solution of either ^{12}C or ^{13}C glucose for 10 days and then propleural plates were dissected out for total RNA extraction (Additional file 1: Fig. S1). Control feeding experiments demonstrated that a fluorescently labelled glucose-water diet was not transferred to the surface of the propleural plate region of the ants during feeding, and the ants were only ever observed to feed using their mandibles, such that their propleural plates never came into direct contact with the liquid diet (Additional file 1: Fig. S2).

Following cDNA synthesis, 16S rRNA gene amplicon sequencing showed that filamentous actinomycetes dominate the propleural plate samples, making up 76.6 % and 78.0 % of the total, unfractionated, cDNA samples from ^{12}C and ^{13}C fed ants, respectively (Fig. 1). The most abundant bacterial genera were *Pseudonocardia*, 35.8% and 38.1% in ^{12}C and ^{13}C samples respectively, and *Streptomyces*, 19.7% and 20.5%, respectively. *Wolbachia* made up 22.8% and 19.6%, respectively. *Wolbachia* are known to be associated with the thoracic muscles of *A. echinatior* worker ants where they may have an unspecified mutualistic function [45, 46]. We conclude that these reads came from the trace amount of residual ant tissue on the dissected propleural plates and do not consider them further. More than 95% of the *Pseudonocardia* 16S rRNA gene reads in unfractionated RNA samples were identical in sequence to a single *P. octospinosus* mutualist strain [18, 32]. The presence of *Streptomyces* and other actinomycete bacteria is consistent with the interpretation of previous studies that environmentally acquired, antibiotic-producing actinomycetes can establish in the cuticular microbiome [36-40, 47], despite these large workers having first been inoculated with the vertically transmitted symbiont *Pseudonocardia* [18].

Caesium trifluoroacetate density gradient ultracentrifugation was used to separate the ^{13}C-labelled "heavier" RNA from the un-labelled ^{12}C "lighter" RNA within the ^{13}C-fed samples (Additional file 1: Fig. S1). RNA samples from the control ^{12}C dietary treatment also underwent density gradient ultracentrifugation. The resulting gradients were fractionated by buoyant density ultracentrifugation, and cDNA from each fraction was used in quantitative RT-

PCR reactions (Additional file 1: Figs. S3 & S4). This demonstrated that 16S rRNA gene transcripts had shifted to higher buoyant densities under the ^{13}C dietary treatment (Additional file 1: Fig. S3). A peak in transcripts was detected at an average buoyant density of 1.789 g ml^{-1} (± 0.003 SD) under the ^{12}C treatment, but this had shifted to a significantly higher buoyant density (1.797 g ml^{-1} ± 0.001, $P = 0.016$ in a two-sample t-test) under the ^{13}C dietary treatment (Additional file 1: Fig. S4). This is consistent with the heavier ^{13}C isotope being incorporated into the RNA of cuticular bacteria, due to the metabolism of labelled host resources (Additional file 1: Fig. S4).

Fractions spanning the peaks in transcript number were selected for 16S rRNA gene amplicon sequencing (Additional file 1: Fig. S4). The relative abundances of taxa identified by sequencing were further normalised using the percentage of 16S rRNA gene transcripts detected in each fraction in the qPCR experiments; this was to account for differences in the absolute abundance of 16S rRNA gene transcripts detected in each fraction, and also to facilitate the comparison of replicates within and across treatments, which differed in the total amount of RNA extracted. Sequencing confirmed that transcripts from actinobacterial genera had shifted to higher buoyant densities under the ^{13}C treatment (Fig. 2A, B and C). For example, the abundance of the vertically transmitted *Pseudonocardia* symbiont tracked changes in the total number of 16S rRNA gene transcripts that had been identified using qPCR (Fig. 2A, Additional file 1: Fig. S4). Specifically, *Pseudonocardia* sequences were detected at an average relative abundance of 36.30% (±7.22) in the peak fractions of the ^{13}C treatment (average buoyant density of 1.797 g ml^{-1} ± 0.001, Fig. 2A) — these fractions contained an average of 66.45% (±12.34) of the total number of 16S rRNA gene transcripts identified within a sample (Additional file 1: Fig. S4), giving a mean normalised abundance of 23.57±1.67 (Fig. 2A). Although *Pseudonocardia* sequences were also detected in fractions of equivalent buoyant density under the ^{12}C treatment (Fig. 2A), these fractions contained less than 2% of the total number of 16S rRNA gene transcripts within these samples (Additional file 1: Fig. S4); hence a mean normalised abundance of 0.78 ± 1.29 was recorded (Fig. 2A). The abundance of *Pseudonocardia* transcripts instead peaked at a significantly lower buoyant density (1.789 g ml^{-1} ± 0.003, $P = 0.016$) under the ^{12}C treatment.

In addition to *Pseudonocardia*, horizontally acquired taxa, including *Streptomyces* and *Microbacterium*, also showed similar shifts to higher buoyant densities under the ^{13}C treatment and were abundant in peak fractions of ^{13}C samples (Fig. 2B and C). For example, *Streptomyces* had an average normalised abundance of 12.790 ± 2.758 in peak fractions of the ^{13}C samples.

This indicates that ant-derived resources were not solely available to the *Pseudonocardia*, which would otherwise have dominated the ^{13}C heavy fractions, but are available to, and taken up by, all bacteria on the cuticle.

The frequency of *Wolbachia* also shifted to heavier fractions under the ^{13}C heavy treatment (Fig. 2D). Since *Wolbachia* are extracellular muscular tissue symbionts in this particular symbiosis [45], this finding supports the interpretation that resources were supplied to cuticular bacteria by the ant hosts and not taken directly from the glucose water. This interpretation is also backed by isotope ratio mass spectrometry (IRMS), which showed that surface-washed ants incorporate a significant amount of the ^{13}C from their glucose diet into their bodies (Additional file 1: Fig. S5), and by direct fluorescent microscopy demonstrating that the glucose water was not transferred to the propleural plate (Additional file 1: Fig. S2). Note that abundances of all other taxa become ca. 20% and ca. 50% higher after excluding *Wolbachia* in the ^{12}C and ^{13}C treatment, respectively (Fig. 2), i.e. when considering only the cuticular microbiome.

Antibacterial BGCs are expressed by *Pseudonocardia* on the ant cuticle. We previously generated high-quality genome sequences for five *Pseudonocardia octospinosus* and five *P. echinatior* strains isolated from *Acromyrmex echinatior* ant colonies and identified several BGCs (biosynthetic gene clusters) in each of their genomes that are associated with antimicrobial activity [32]. To establish if these BGCs are expressed *in vivo* on the ant cuticle, total RNA was extracted and sequenced from the propleural plates of ants in the captive colonies Ae088 (which hosts a vertically transmitted *P. echinatior* strain) and Ae1083 (which hosts a *P. octospinosus* strain) (Additional file 1: Table S1 [32, 37, 47-56]). A single RNA extraction was carried out for each colony, with each sample consisting of the pooled propleural plates of 80 individual ants. RNA samples were sequenced, and the resulting reads were quality filtered and mapped to their corresponding *Pseudonocardia* reference genomes [32] (Additional file 1: Table S2). Both *Pseudonocardia* species showed very similar patterns of gene expression *in vivo*, with genes involved in the production of secondary metabolites, including antibiotics (as classified by KEGG) being expressed at similar levels by both *Pseudonocardia* strains on the cuticle of *A. echinatior* ants (Additional file 1: Fig. S6).

BGCs that are shared by the *P. octospinosus* and *P. echinatior* strains (Additional file 1: Table S3 [32]) displayed remarkably similar patterns of *in situ* expression on the propleural plates (Fig. 3A). For both *Pseudonocardia* species, the most highly expressed BGCs encoded

proteins responsible for the synthesis of the compound ectoine and a putative carotenoid terpene pigment (cluster D and F, Fig. 3A). Such compounds are known to provide protection against abiotic stressors such as desiccation and high concentrations of free radicals which are often associated with biofilms [57-59]. Also expressed on the propleural plates is a shared BGC encoding a putative bacteriocin (Cluster E, Fig. 3A), which belongs to a family of ribosomally-synthesized post-translationally modified peptide (RiPP) antibiotics produced by many species of bacteria [60-62]; these are known to prevent the formation of biofilms by other microbial species [60, 63]. In contrast, a shared Type 1 PKS gene cluster, encoding nystatin-like antifungal compounds [32, 37], had very low expression in the *P. echinatior* strain and was not expressed at all in the *P. octospinosus* strain (cluster C, Fig. 3A). This suggests that additional cues, such as direct exposure to *E. weberi* may be required to activate this BGC, since both *Pseudonocardia* strains produce inhibitory antifungals when confronted with *E. weberi in vitro* (Additional file 1: Fig. S7). A *Pseudonocardia* strain isolated from *Acromyrmex* ants has also previously been shown to produce nystatin-like compounds *in vitro* [37]. The most highly expressed BGCs unique to *P. echinatior* (cluster P, Fig. 3C) or *P. octospinosus* (cluster J, Fig. 3B) are both predicted to encode bacteriocins.

Taken together, the results of the RNA-SIP and RNA sequencing experiments are consistent with both previous empirical research [18, 33] and the screening hypothesis [12, 13]: the ant host provides public resources to its cuticular microbiome via glandular secretions [41] for which colonising ectosymbionts may compete. This is always after the native *Pseudonocardia* has established and gained dominance, which creates a demanding cuticular environment for any additional strain to invade.

***Pseudonocardia* antibacterials create a demanding environment for non-antibiotic-producing bacteria**. Next we compared the growth rates of antibiotic-producing *Streptomyces* strains and non-antibiotic-producing bacteria on antibiotic-infused and control media. All strains were isolated from soil or fungus-growing ant nests (Additional file 1: Table S1). The antibiotic-infused media were created by growing lawns of 17 *Pseudonocardia* isolates (Additional file 1: Table S1) on SFM agar, while control media were inoculated with 20% glycerol. After a six-week incubation period, the agar medium was flipped to reveal a surface for colonisation. The non-producer strains grew more quickly on the non-demanding control media while the antibiotic-producers grew more quickly on the demanding *Pseudonocardia*-infused media, producing a highly significant statistical interaction effect ($n = 975$, $\chi^2 = 45.86$,

df = 2, $p < 0.0001$; Fig. 4). There was also a significant main effect of *Pseudonocardia* genotype, with both non-producers and producers exhibiting a lower growth rate on *P. echinatior* (Ps2)-infused media than on *P. octospinosus* (Ps1)-infused media (linear mixed-effects model, n = 915, $\chi^2 = 24.55$, df = 1, $p < 0.0001$, control-media data omitted for this analysis). This outcome is consistent with the observation by Andersen *et al.* [18] that *Acromyrmex* colonies hosting Ps2-dominated cuticular microbiomes were less prone to secondary invasion by other bacteria.

To test the hypothesis that producer strains are generally resistant to antibiotics, which would confer competitive superiority in an antibiotic-infused host environment [12], we grew ten producer strains (all *Streptomyces* spp.) and ten non-producer strains (Additional file 1: Table S1) in the presence of eight different antibiotics (Additional file 1: Table S4), representing a range of chemical classes and modes of action. After seven days, Lowest Effective Concentration (LEC, lowest concentration with inhibitory effect) and Minimum Inhibitory Concentration (MIC, lowest concentration with no growth) scores were assigned on a Likert scale of 1–6, where a score of 1 was no resistance and a score of 6 was resistance above the concentrations tested [65]. Antibiotic-producer strains exhibited greater levels of resistance, measured by both LEC (Wilcoxon two-sided test, W = 94.5, $p = 0.0017$) and MIC scores (W = 80, $p = 0.0253$); *p*-values corrected for two tests (Fig. 5).

We also performed growth-rate experiments and measured antibiotic resistance profiles with resident non-antibiotic-producing strains that had been directly isolated from cuticular microbiomes. These strains had significantly slower growth rates overall, even on control media without antibiotics, suggesting that these strains are just transient environmental contaminants (Additional file 1: Fig. S8). These resident non-producer strains also demonstrated high levels of resistance as expected (Additional file 1: Fig. S9), given that they had been isolated from ant cuticles.

***Pseudonocardia* antibacterials allow *Streptomyces* to competitively exclude non-antibiotic-producing bacteria**. Finally, to test whether producer strains have a competitive advantage in the demanding environment created by *Pseudonocardia*, we pairwise-competed two of the *Streptomyces* producer strains, named S2 and S8 (Additional file 1: Table S1), against each of 10 environmental non-producer strains on normal and on antibiotic-infused media. In the latter case, *Pseudonocardia* was again grown on agar plates before turning the agar over and coinoculating producer and non-producer test strains. On normal growth media,

Streptomyces were more likely to lose to non-producers, but on *Pseudonocardia*-infused media, *Streptomyces* were more likely to win (general linear mixed-effects model; S8 on Ps1-infused media: $n = 129$, $\chi^2 = 103.6$, $df = 1$, $p < 0.0001$; S2 on Ps2-infused media: general linear mixed-effects model, $n = 94$, $\chi^2 = 87.9$, $df = 1$, $p < 0.0001$; Fig. 6).

Discussion

We tested screening theory using the external (cuticular) microbiome of the leaf-cutting ant *Acromyrmex echinatior* as an experimental model. We used RNA-SIP to show that an animal host is directly feeding its microbiome (Fig. 2). We further show that the resource is public, meaning that the resource is used for growth not only by vertically transmitted *Pseudonocardia* but also by multiple species of environmentally acquired bacteria on the ant cuticle (Fig. 2). We then demonstrated, in two separate ant colonies, that both *P. octospinosus* and *P. echinatior* strains express antibacterial biosynthetic gene clusters (BGCs) on the ant cuticle (Fig. 3). We next showed that the two species of actinobacteria have broad-spectrum antibacterial activity against environmental isolates *in vitro* and, importantly, have a weaker effect on *Streptomyces* than on non-producers (Fig. 4), consistent with these *Streptomyces* species being resistant to a range of antibiotics (Fig. 5), which is typical for this genus. Finally, we used *in vitro* competition experiments to demonstrate that *Streptomyces* species can competitively exclude faster-growing bacteria that do not make antibiotics, but only when the competing species are grown on media infused with *Pseudonocardia* metabolites (Fig. 6).

Although feeding treatments for the RNA-SIP experiment were conducted over a short time-frame (ten days), it is possible that some of the bacterial symbionts acquired resources indirectly, by using labelled metabolites produced by other microbes that were feeding directly on the ant-derived resources. However, cross-feeding is still consistent with the food resource being public, and thus consistent with competition-based screening, since multiple bacterial species, including horizontally acquired actinobacteria, are still taking up host-supplied resources for growth, albeit indirectly, thus fuelling competition amongst species for host space.

Taken together, these results are consistent with the hypothesis that competition-based screening is a plausible mechanism for maintaining the integrity of the co-adapted mutualism between the leaf-cutting ant farming symbiosis and its defensive microbiome, predicted to be conditional on the vertically transmitted *Pseudonocardia* symbiont always being the first to

establish and create a demanding environment. This priority establishment is invariably the case because callow large workers are inoculated by their nestmates within 24 hours of emerging from their pupae [34]. *Pseudonocardia* is also never competitively excluded from the microbiome, as predicted by Scheuring & Yu [12] and empirically shown by Andersen *et al.* [18]. Indeed, initial advantages of early colonization and nutrients allow *Pseudonocardia* to form a dense growth before additional microorganisms can colonise the ant cuticle. The new results reported here illustrate the tractability of the cuticular leaf-cutting ant microbiome, which is accessible to experimentation and for which the adaptive benefit to the ant hosts is clearly defined and explicitly testable: defence against specialized *Escovopsis* pathogens and colony collapse [3, 25, 37, 66]. Our present results are consistent with our previous hypothesis that the vertical transmission of *Pseudonocardia* results in *Streptomyces* strains being superior contenders for secondary acquisition [12].

An alternative hypothesis to screening is that the ants selectively acquire additional antibiotic-producing bacteria via a lock-and-key mechanism, in the same way that leguminous plants recognise *Rhizobium* symbionts via species-specific Nod-factor signalling molecules [67]. However, lock-and-key signalling requires tight coevolution between all candidate symbiont and host lineages (see [68] for one model), which could be true for the *Acromyrmex*-associated *Pseudonocardia* species but is highly unlikely for the other genera across the phylum Actinobacteria that can become established on the ant cuticle (Fig. 1). In contrast, legumes associate with only one genus of root-nodule symbionts, *Rhizobium*.

The petri-dish competition experiments have the important advantage of allowing unambiguous scoring of wins, losses, and draws on media with and without *Pseudonocardia*. However, future work should focus on adding realism, since on the cuticle, competition is taking place among multiple species, with variation in colonization order, the cuticular microenvironment, and resource provisioning rates [13]. However, although it is possible to prevent the establishment of *Pseudonocardia* on newly eclosed workers [34], the technical challenge will be to score relative species abundances (i.e. winners and losers) from sequencing datasets, in the face of cryptic species biases (see [69] for a discussion of this problem and [70] for a potential solution). A complementary approach would be to compare competition *in vitro* and *in vivo* with wild-type and knock-out strains of *Pseudonocardia* that are unable to produce the antimicrobial compounds observed in RNA-seq experiments. However, such an experiment would require extensive genetic modification, which has so far proven very challenging in *Pseudonocardia.*

Although competition has not been demonstrated via addition or removal experiments, we have shown clear resource-use overlap via the RNA-SIP experiment (Fig. 1) and the capacity for competitive exclusion via the Petri-dish experiment (Fig. 6). Combined with the capacities for exponential growth and for antibiotic production in the *Streptomyces* strains, we have a strong expectation of both scramble and interference competition in the attine cuticular microbiome.

The nature and origin of the host-derived resources remain elusive. Previous studies have observed that *Pseudonocardia* grows in or above specialized cavities on the ant cuticle, called foveae, that are underlain by structures that appear to be exocrine glands [41]. However, it has not been experimentally confirmed that these glands are the source of resources supplied to the cuticular microbiome. Another study has shown that metapleural gland secretions (the only other exocrine secretion that could reasonably spread over the entire cuticle) have no influence on the early exponential growth phase of *Pseudonocardia* in callow ants [71]. Closure of these glands was shown to influence the growth of *Pseudonocardia* in older ants, but it was unclear if artificial manipulations had compromised other aspects of ant health in this instance [71].

There are several emerging techniques that might be used to locate and identify host-derived substrates in future experiments. For example, high resolution secondary ion mass spectrometry imaging (NanoSIMS), combined with fluorescent *in situ* hybridisation (FISH) can be used to directly visualize the assimilation of stable isotopes by different bacterial taxa [72]. This technique has been used to visually track the bacterial metabolism of labelled compounds secreted by the mouse intestinal mucosa [73]. Similarly, Raman microspectroscopy creates a chemical fingerprint of a molecule or system and can identify compounds that have incorporated heavy isotopes via the spectral shifts that take place [74]. Techniques such as matrix-assisted laser desorption/ionisation time-of-flight (MALDI-TOF) imaging mass spectrometry could also be applied in a similar way and, although extremely challenging to carry out, has been used to image the distribution of an antifungal compound over the surface of *A. echinati*or ants [39].

Our results show that competition-based screening is a plausible mechanism for the acquisition of a diverse, antibiotic-producing microbiome. The natural follow-on question is whether this mechanism represents an *Acromyrmex* adaptation that improves defense against pathogens. We do know that *Streptomyces* species isolated from *Acromyrmex* ants can produce antifungals that inhibit the growth of *Escovopsis in vitro* [37, 39, 47, 75], but a direct

test would require experimental removal and addition of *Streptomyces* (and/or antibiotic gene knock-outs), which so far have posed significant technical challenges. However, as noted above, *Streptomyces* symbionts have rarely been found on the callow workers [18] that tend the fungus garden [35]. Thus, the screening effect shown in our experiments might be an epiphenomenon of the mutualism between *Pseudonocardia* and *Acromyrmex*. In this case, the leafcutter ant system can be thought of as a tractable model for a screening phenomenon that may have adaptive significance elsewhere. Alternatively, the adaptive benefit of the extra actinobacterial species could be that they improve the protection of foraging workers from bacterial and fungal infections acquired outside the colony, thereby also indirectly protecting workers that interact more extensively with the fungus garden. Given that bacterial competition is known to stimulate antimicrobial export *in vitro* [76, 77], having multiple strains on individual ants may then be beneficial by stimulating the production of multiple different antimicrobial compounds. Indeed, Schoenian et al. [39] have directly visualized the production of the antimicrobial valinomycin by a *Streptomyces* strain on the cuticles of mature *Acromyrmex* workers. We also hypothesise that continuous competition against antibiotic-producing competitors may select against *Pseudonocardia* losing costly antimicrobial production genes as a side effect of its domestication by attine ants.

Our results are of broad significance because competition-based screening provides a mechanistic explanation for microbiomes to be evolutionary stable ecosystems-on-a-leash [8]; here, the host leash works by fomenting and biasing competition, via the combination of public resources and a vertically transmitted antibiotic-producing symbiont, to favour the establishment of antibiotic-producing bacteria [12]. This perspective is consistent with the idea that host-associated microbiomes can have both core members that co-adapt with host environments and non-adapted but still mutualistic members. Studies in other symbioses appear to support this dual evolutionary and ecological view [14, 16, 17], both for an array of mutualistic symbioses with multicellular partners and for microbiomes more specifically. For instance, the actinomycete *Bifidobacterium longum* subsp. *infantis* dominates the guts of human neonates [11, 78]. In this case, the *Bifidobacterium* is an early coloniser because it is transmitted vertically from mother to child, and *Bifidobacterium* consumes a range of oligosaccharides provided in human breast milk to build up a large enough population that it can competitively exclude pathogen colonisers. We hypothesise that *Bifidobacterium* could act like *Pseudonocardia* and selectively favour the establishment of other *Bifidobacterium*

species in the gut, at least until weaning. Similarities may also be seen in the ant species, *Lasius fuliginosus*, which stabilizes its carton-nest structures through the growth of a remarkably predictable community of fungi [79]. Experiments have shown that antimicrobial substances, originating from the ant body parts, are tolerated by these fungal associates and support their growth, enabling them to outcompete other species of doubtful loyalty to the symbiosis in the nest structure [79]. Similar processes may also play out during the establishment of plant-root microbiomes [80-83] and could be open to manipulation in efforts to improve crop yields [84].

Future work on the *Acromyrmex* model system should include characterising the antibacterial molecules made by the symbiotic *Pseudonocardia* strains *in vitro* and *in vivo* and matching these compounds to the BGCs expressed on the ants. This will be challenging because ant-derived *Pseudonocardia* strains grow poorly on agar plates and rarely in liquid culture. Additionally, Imaging Mass Spectrometry has, as yet, not been possible on the ants themselves.

Methods

Ant colony collection and maintenance. Colonies of *A. echinatior* (Hymenoptera, Formicidae, Attini) were collected from the Gamboa area of the Soberania National Park, Panama, between 2001 and 2014. Colonies Ae1083 and Ae088 (Additional file 1: Table S1) were maintained under controlled temperature conditions (25ºC) at UEA and fed a daily diet of bramble and laurel leaves. Additional colonies were maintained at the University of Copenhagen in rearing rooms at ca 25ºC and 70% relative humidity, where they were fed with bramble leaves and occasional supplements of apple and dry rice.

RNA Stable Isotope Probing.

RNA SIP ^{13}C feeding experiment. Six replicate groups of 22 mature worker ants with visible bacterial growth on their propleural plates were selected from colony Ae1083 (Additional file 1: Table S1) and placed into 9cm petri dishes containing a 2x2 cm square of cotton wool soaked in water. Following 24 hours of starvation, three replicate groups of 22 ants were supplied with 300 µl of a 20% ^{13}C glucose solution (w/v, Sigma Aldrich) and the remaining three groups were supplied with 300 µl of a 20% ^{12}C glucose solution (w/v, Sigma Aldrich) for 10 days. Glucose solutions were supplied to ants in microcentrifuge tube caps and were

refreshed every three days. To confirm uptake of the ^{13}C isotope by ants fed on the ^{13}C labelled diet, a further 5 ants were fed on each type of glucose diet; these were submitted for Isotope Ratio Mass Spectrometry (IRMS) analysis, which enables the relative abundance of each stable isotope (^{13}C and ^{12}C) to be quantified in a sample.

Isotope ratio mass spectrometry analysis. The ^{13}C composition of ants fed on a ^{13}C-labelled diet was determined by using a coupled Delta plus XP Isotope Ratio Mass Spectrometer/Flash HT Plus Elemental Analyser (Thermo Finnigan) in the University of East Anglia Analytical Facility. Ants were fed on a 5% glucose solution (w/v) for 10 days; five ants were fed a ^{13}C glucose solution and five were fed on a ^{12}C glucose solution. After 10 days, ants were washed once in 70% ETOH, then sequentially in sterile dH_2O before drying on filter paper. The ants were then flash frozen and stored at -80°C until being placed in a ScanVac Coolsafe freeze dryer for 5 days. Each ant was then put into an individual 75 µl tin capsule (Elemental Microanalysis); capsules were loaded into an automatic sampler and completely converted to CO_2, N_2 and H_2O through combustion in an excess of oxygen (oxidation was carried out at 1020°C, followed by reduction at 650°C). Nitrous oxides formed during combustion were reduced using Cu. Helium was used as a carrier gas. After passing through a water trap ($MgClO_4$), the gases were separated chromatographically on an isothermal GC column (Thermo PTFE, 0.8m, 50°C); the resulting peaks sequentially entered the ion source of the Isotope Ratio Mass Spectrometer. Gas species were then measured using a Faraday cup universal collector array, with masses of 44, 45 and 46 being monitored for the analysis of CO_2. Casein and collagen were used to calibrate the system and normalize the data post run; these standards have been calibrated against international certified standards and have an assigned $\delta^{13}C$ value. Empty tin capsules were used as blanks. Each sample was analysed in triplicate. The ^{13}C content of samples was reported as the ^{13}C atom percent, which was calculated using the following formula:

$$(^{13}C/^{12}C+^{13}C)*100$$

Fluorescent microscopy of ant feeding habits. To confirm that the glucose water diet did not spread over the ant cuticle, a 20% glucose solution labelled with non-toxic fluorescent green drain tracing dye (Hydra) was fed to ants. Five mg ml^{-1} of dye was added to a 20% glucose solution, of which 300 µl was supplied to ants in the cap of an Eppendorf. Ants were

sampled just after taking a feed, and after 6 and 24 hours of being exposed to the dye, to trace the spread of the solution over time. After sampling, ants were carefully fixed on their backs and brightfield and fluorescent images were acquired using a Zeiss M2 Bio Quad SV11 stereomicroscope (Additional File 1: Fig. S2). The samples were illuminated either with a halogen lamp (brightfield) or a 100W Hg arc lamp (fluorescence) and reflected-light images were captured with an AxioCam HRc CCD camera and AxioVision software (Carl Zeiss, Cambridge, UK). Green fluorescence was excited with light passed through a 470 nm filter (40 nm bandpass) and the emission was collected through a 525 nm filter (50 nm bandpass).

Cuticular dissection and RNA extraction. At the end of the 10-day feeding experiment, the propleural plates of the propleura were removed from the ventral exoskeleton using a dissection microscope and fine sterile tweezers. Propleural plates from each of the 22 ants in each dietary group were placed together in lysis matrix E tubes (MP Biomedicals) on dry ice, before being snap frozen in liquid nitrogen. A modified version of the Qiagen RNeasy Micro Kit protocol was used for all RNA extractions. Briefly, 700 µl of RLT buffer (with 1% beta mercaptoethanol) was added to each lysis matrix E tube before the samples could thaw. Tubes were then placed in a FastPrep-24™ 5G benchtop homogenizer (MP Biomedicals) and disrupted for 40 seconds at 6 m/s. Samples were then centrifuged for 2 minutes at 13’000 rpm and the supernatant was collected into a QIAshredder tube. This was centrifuged for 2 minutes at 13,000 rpm to homogenize the lysate. The resulting flow-through was mixed vigorously with 700 µl acidic phenol chloroform, then allowed to rest for 3 minutes at room temperature before centrifugation for 20 minutes at 13,000 rpm. The upper phase was then collected, and a 50% volume of 96% ethanol was added. The mixture was then placed into a minelute column supplied with the Qiagen RNeasy Micro Kit. The kit protocol (including the on-column DNase I treatment) was then followed through to elution of the RNA, at which point 50 µl of RNase free water (heated to 37°C) was added to the column membrane and incubated at 37°C for 5 minutes, before centrifuging for one minute at 13,000 rpm to elute the RNA. To remove any remaining DNA, RNA was treated with the turbo DNase kit (Invitrogen): 5 µl of 10x buffer and 2 µl of Turbo DNase was added to 50 µl of RNA and incubated at 37°C for 25 minutes. RNA was then purified using the Qiagen Micro RNA Kit clean-up protocol. The quantity and purity of all RNA samples was checked using a nanodrop spectrophotometer and a Qubit™ RNA HS assay kit (Invitrogen™).

Density gradient ultracentrifugation and fractionation. Density gradient ultracentrifugation was carried out to separate ^{13}C labelled ("heavy") from un-labelled ("light") RNA within the same sample. To make one complete gradient solution for the ultracentrifugation of one RNA sample, 4.5 ml of caesium trifluoroacetate (CsTFA, ~2 g ml^{-1}, GE Healthcare, Munich, Germany) was added to 850 µl of gradient buffer and 197.5 µl formamide. Gradient buffer was made using an established protocol [85]. Following this, 270 ng of RNA from one replicate sample was added to the gradient solution and the refractive index (R.I) of a 60 µl aliquot was measured using a refractometer (Reichert Analytical Instruments, NY, USA). The R.I was then normalized to 1.3725 (approximately 1.79 g ml^{-1} CsTFA). Samples underwent ultracentrifugation in a Beckman Optima XL-100K ultracentrifuge for 50 hours at 20°C, 38,000 rpm with a vacuum applied, using a Vti 65.2 rotar (Beckman Coulter, CA, USA). Deceleration occurred without brakes. Following centrifugation, samples were divided into 12 fractions using a peristaltic pump to gradually displace the gradient, according to an established protocol [44]. The R.I of fractions was measured to confirm the formation of a linear density gradient. RNA was precipitated from fractions by adding 1 volume of DEPC-treated sodium acetate (1M, pH 5.2), 1 µl (20 µg) glycogen (from mussels, Sigma Aldrich) and 2 volumes of ice cold 96% ethanol. Fractions were incubated over night at -20°C then centrifuged for 30 minutes at 4°C at 13,000 x g, before washing with 150 µl of ice cold 70% ethanol and centrifuging for a further 15 minutes. Pellets were then air-dried for 5 minutes and re-suspended in 15 µl of nuclease free water.

Quantifying 16S rRNA gene copy number across RNA SIP fractions. The RNA in each fraction was converted to cDNA by following the manufacturer's instructions for Superscript II (Invitrogen) with random hexamer primers (Invitrogen). 16S rRNA gene copy number was then quantified across cDNA fractions using qPCR. For this, 1 µl of either template cDNA, standard DNA, or dH_2O as a control, was added to 24 µl of reaction mix containing 12.5 µl of 2x Sybr Green Jumpstart Taq Ready-mix (Sigma Aldrich), 0.125 µl of each of the primers PRM341F and 518R (Additional File 1: Table S1), 4 µl of 25 mM MgCl2, 0.25 µl of 20 µg $µl^{-1}$ Bovine Serum Albumin (Sigma Aldrich), and 7 µl dH_2O. Sample cDNA, standards (a dilution series of the target 16S rRNA gene at known quantities), and negative controls were quantified in duplicate. Reactions were run under the following conditions: 95°C for 10 mins; 40 cycles

of 95°C for 15 sec, 55°C for 30 sec, and 72°C for 30 sec; plate read step at 83.5°C for 10 seconds (to avoid primer dimers); 96°C for 15 sec; 100 cycles at 55°C-95°C for 10 secs, ramping 0.5°C per cycle, followed by a plate read. Reactions were performed in 96-well plates (Bio-Rad). The threshold cycle (CT) for each sample was then converted to target molecule number by comparing to CT values of a dilution series of target DNA standards. These values were further converted to percentages based on the total number of 16S rRNA gene transcripts identified in each sample.

Sequencing and analysis. PCR was used to amplify the 16S rRNA gene in each of the fractions that spanned the peaks in 16S rRNA gene copy number, identified via qPCR. This was done using the primers PRK341F and 518R (Additional file 1: Table S1). One unfractionated sample was also created for ants under each of the ^{13}C or ^{12}C dietary treatments, by pooling equal quantities of unfractionated cDNA from each of the 3 replicate groups and using this as template for PCR amplification. The resulting PCR products were purified using the Qiagen MinElute™ gel extraction kit and submitted for 16S rRNA gene amplicon sequencing using an Illumina MiSeq at MR DNA (Molecular Research LP), Shallowater, Texas, USA. Sequence data was then processed by MR DNA using their established pipeline (as described in [86, 87]). As part of this pipeline, paired-end sequences were merged, barcodes were trimmed, and sequences of less than 150 bp and/or with ambiguous base calls were removed. The resulting sequences were denoised, and OTUs were assigned by clustering at 97% similarity. Chimeras were removed, and OTUs were taxonomically assigned using BLASTn against a curated database from GreenGenes, RDPII, and NCBI [88]. Plastid-like sequences were removed from the analysis. Upon receipt of the 16S rRNA gene sequencing data from MR DNA, OTU assignments were verified using QIIME2 and BLASTn, and statistical analysis was carried out using R 3.2.3[89]. OTUs assigned as *Pseudonocardia* were blasted against the 16S rRNA gene sequences for *P. echinatior* and *P. octospinosus* [32] to confirm the relative abundance of each of these vertically-transmitted strains in the samples. All 16S rRNA gene amplicon sequencing data from this experiment has been deposited in the European Nucleotide Archive (ENA) public database under the study accession number PRJEB32900 [90]. Relative abundances were normalised using the qPCR data on the total 16S rRNA gene transcripts occurring within a fraction. Specifically, the following formula was used: (R*P)/100, where R is the relative abundance of a taxon and P is the percentage of 16S rRNA gene transcripts detected in that particular fraction of a sample.

Detecting the expression of *Pseudonocardia* BGCs *in situ*.

RNA extraction and sequencing from ant propleural plate samples. The propleural plates of *Acromyrmex echinatior* ants were dissected (as described above) from individual mature worker ants that had a visible growth of *Pseudonocardia* bacteria on their cuticle. A pool of 80 ant cuticles were sampled from each of the colonies Ae1083 and Ae088, respectively (Additional file 1: Table S1), after which RNA was extracted as described above. The quantity, purity and integrity of all RNA samples was checked using a nanodrop spectrophotometer and Qubit™ RNA HS assay kit (Invitrogen™), as well an Experion™ bioanalyser with a prokaryotic RNA standard sensitivity analysis kit (Bio-Rad, California, USA). One μg of RNA from each of the propleural plate samples was sent to Vertis Biotechnologie AG (Freising-Weihenstephan, Germany) where samples were processed and sequenced using an RNA sequencing approach [as described in 91]. Single-end sequencing (75 bp) was performed using an Illumina NextSeq500 platform. All sequencing reads have been deposited in the ENA public database under the study accession number PRJEB32903 [92].

Processing of reads generated from RNA sequencing experiments. The quality of Illumina sequences (returned from Vertis Biotechnologie AG) was assessed using the program FastQC (Babraham Institute, Cambridge, UK), before using TrimGalore version 0.4.5 (Babraham Institute, Cambridge, UK) to trim Illumina adaptors and low quality base calls from the 3' end of reads (an average quality phred score of 20 was used as cut-off). After trimming, sequences shorter than 20 base pairs were discarded. Trimmed files were then aligned to the reference genome for *Acromyrmex echinatior* (Additional File 1: Table S1 [55]), and the appropriate *Pseudonocardia* genome (either Ae707 for the sample from colony Ae1083, or Ae706 for the sample from colony Ae088 [32]; see Additional File 1: Table S1 for genome information). All alignments were done using the splice-aware alignment program HiSat2 [93] with the default settings. For each cuticular sample, reads that had mapped successfully to their respective *Pseudonocardia* genomes (Additional File 1: Table S2) were then mapped back to the ant genome (and vice versa) to check that reads did not cross-map between the two genomes (i.e that they were either uniquely ant or bacterial reads) - reads that did not cross-map were retained for downstream analysis. Following alignment, the program HTSeq [94] was used to count mapped reads per annotated coding sequence (CDS) using the General Feature Format

(GFF) file containing the annotated gene coordinates for each reference genome. Reads that mapped to multiple locations within a genome were discarded at this point and only uniquely mapped reads were used in the counting process. Read counts per CDS were then converted to reads per kilobase of exon model per million reads (RPKM) by extracting gene lengths from the GFF file. Converting reads to RPKM values normalizes counts for RNA length and for differences in sequencing depth, which enables more accurate comparisons both within and between samples [95].

Expression analysis. In order to investigate the expression levels of different functional groups of genes, protein sequences of every annotated gene in each *Pseudonocardia* genome [32] (Additional file 1: Table S1) were extracted and uploaded to BlastKOALA [96]. Assigned K numbers were classified into five main KEGG pathway categories (and their associated sub-categories) using the KEGG Pathway Mapper tool. Each gene, with its associated K number and category assignments, was then matched to its RPKM value from the RNA sequencing dataset so that the expression levels of different KO categories could be established. To investigate the expression of biosynthetic gene clusters (BGCs) by *Pseudonocardia* on the ant cuticle, reference genome sequences for *P. octospinosus* and *P. echinatior* (Additional file 1: Table S1 [32]) were uploaded to antiSMASH version 4.0, which predicts the presence and genomic location of BGCs based on sequence homology to known clusters [97]. RPKM values were then generated for each predicted BGC, based on the length of the predicted cluster and read counts for genes situated within it.

Isolation of *Pseudonocardia* and *Escovopsis* bioassays. The *Pseudonocardia* strains PS1083 and PS088 (Additional file 1: Table S1) were isolated from the propleural plates of individual large *Acromyrmex echinatior* workers taken from colonies Ae1083 and Ae088 (colonies used in RNA-seq experiments, see Additional file 1: Table S1), respectively. Similarly, *Pseudonocardia* strains Ae322, Ae712, Ae280, Ae160, Ae703, Ae702, Ae707, Ae704 and Ae715 were isolated from large worker ants from colonies with the same labels maintained at the University of Copenhagen (these strains were only used for the growth-rate experiments described in the section below). A sterile needle was used to scrape bacterial material off the propleural plates on the ventral part of the thorax; this was then streaked over Soya Flour Mannitol (SFM, Additional File 1: Table S4) agar plates and incubated at 30°C.

Resulting colonies resembling *Pseudonocardia* were purified by repeatedly streaking single colonies onto SFM agar plates. Spore stocks were created using an established protocol [98]. The taxonomic identity of each *Pseudonocardia* isolate was confirmed via colony PCR and 16S rRNA sequencing, as described in Holmes *et al.* [32]. Each resulting sequence was also aligned to both the *Pseudonocardia octospinosus* and *Pseudonocardia echinatior* 16S rRNA gene sequences [32] to reveal their percentage identities to each of the two species.

Antifungal bioassays were carried out using the specialized fungal pathogen *Escovopsis weberi* strain CBS 810.71, acquired from the Westerdijk Fungal Biodiversity Institute (Additional File 1: Table S1). *E. weberi* was actively maintained on potato glucose agar (PGA, Additional File 1: Table S4) at room temperature. Fungal mycelia were transferred to a fresh plate every month. For bioassays, a plug of actively growing mycelium was transferred from PGA plates to the edge of a Glucose Yeast Malt (GYM, Additional File 1: Table S4) agar plate with a growing *Pseudonocardia* colony (strain PS1083 or PS088, Additional File 1: Table S1), using the end of a sterile glass Pasteur pipette. Plates were then left at room temperature for 2 weeks. A zone of clearing around the *Pseudonocardia* colony indicated the presence of antifungal activity. Three replicate experiments (with three replicate bioassay plates per *Pseudonocardia* strain) were carried out, whereby different *E. weberi* starter plates were used as an inoculum.

***In vitro* competition experiments.**

Collection and isolation of bacterial strains. Nineteen strains of *Pseudonocardia* (11 strains of *P. echinatior* and 8 of *Pseudonocardia octospinosus*, Additional file 1: Table S1) were isolated from the cuticles of individual *Acromyrmex echinatior* worker ants across 18 different colonies and genotypes, as described above. Ten of these isolated *Pseudonocardia* strains were previously genome-sequenced by Holmes *et al.* [32]. The 10 environmental antibiotic-producer strains (all in the genus *Streptomyces*) were taken from general collections in the Hutchings lab and are a mixture of isolates from either soil environments or from worker ants taken from captive colonies (Additional file 1: Table S1). The 10 environmental non-producer strains were obtained from the Hutchings lab (two strains) and from the ESKAPE suite (eight strains with varying origins (human skin, soil, etc.)) used to test antibiotic resistance or efficacy in clinical/research settings (Additional file 1: Table S1).

Individual growth-rate experiments. To create the *Pseudonocardia*-infused media, lawns of each of the 19 isolates (Additional File 1: Table S1) were grown, by plating 30 µl of spores (in 20% glycerol) onto 90 mm SFM agar plates (Additional File 1: Table S4). The control plates were inoculated with 20% glycerol only. We incubated these plates at 30 °C for 6 weeks, which ultimately produced confluent lawns from 17 strains that could be included in the experiments (6 Ps1, 11 Ps2). After a six-week incubation period, the agar medium was flipped to reveal a new surface for colonisation. The 10 environmental producer strains and the 10 environmental non-producer strains (Additional File 1: Table S1) were then inoculated onto the plates to compare their growth rates on each type of media. Each of the plates received 10 evenly spaced colonies, with 3 replicates, generating 2 invader types x 17 Ps-media-types x 3 replicates = 102 Ps-infused plates, and 2 invader types x 3 replicates = 6 control plates, for 1020 treatment and 60 control inoculations. Each strain inoculation used 5 µl of solution (approx. 1 x 10^6 cells per ml in 20% glycerol), spotted at evenly spaced positions and without coming into direct contact. All plates were incubated at 30 °C for five days, after which photographs were taken.

Images were processed in Fiji software [99, 100], creating binary negatives (black & white) so automated tools could identify discrete areas of growth (black) and measure growth areas for each invading strain; in the few cases where binary image resolution was insufficient, outlines were added manually before area calculation. 48 producer-inoculated and 57 non-producer-inoculated treatment measurements were excluded because plate condition had deteriorated to become unscorable or they were contaminated, leaving final sample sizes of 1020-48-57= 915 treatment inoculations and 60 controls.

The second growth-rate experiment compared the 10 *Acromyrmex*-resident, non-producer strains with 9 of the environmental producer strains (1 of the 10 inoculations failed to grow). All 19 *Pseudonocardia* strains grew sufficiently to be included in this experiment, and each plate was again inoculated with 10 or 9 evenly spaced colonies. Starting sample sizes were therefore 2 invader types x 19 Ps-media-types x 3 replicates = 114 Ps-infused plates and 2 x 3 = 6 control plates, for 1083 treatment and 57 control inoculations. Fifty producer and 20 non-producer treatment measurements were excluded for the same reasons as above, leaving final sample sizes of 1083-50-20=1013 treatment and 57 control inoculations, scored as above.

Pairwise competition experiment. Experiments were set up to test whether antibiotic-producer strains could win in direct competition against non-producing strains, both on

normal media and on media infused with *Pseudonocardia* secondary metabolites. To create the *Pseudonocardia*-infused media, we plated 30 µl of spores (in 20% glycerol) onto 50 mm SFM agar plates (Additional File 1: Table S4). The control plates were inoculated with 20% (v/v) glycerol only. We incubated these plates at 30 °C for 6 weeks, which ultimately produced confluent lawns. As above, the agar was flipped to reveal a surface open for colonisation. Environmental producers and non-producers were then coinoculated onto these media (as well as on control media with no *Pseudonocardia* present), and we measured the outcome of competition as a win, loss or draw. To keep the number of tests manageable, we used two combinations of *Pseudonocardia*-infused media and *Streptomyces*: *Pseudonocardia octospinosus* (strain Ae707-CP-A2) + *Streptomyces* S8, and *Pseudonocardia echinatior* (strain Ae717) + *Streptomyces* S2 (Additional File 1: Table S1). We competed the two *Streptomyces* strains (S2, S8) against the 10 environmental non-producer strains (20 pairings). Each *Strepromyces* strain was prepared as 10^6 spores ml^{-1} in 20% glycerol. Each non-producer strains was grown overnight in 10 ml of Lennox broth (Additional File 1: Table S4), before subculturing (1:100 dilution) into 10 ml of fresh Lennox, and incubating at 37 °C for 3-4 hours. The OD_{600} was then measured, assuming that OD_{600} of 1 represented 8×10^9 cells. Similar dilutions of 10^6 cells per ml were made for each non-producer strain in 20% (v/v) glycerol, after which producer and non-producer preparations were mixed at a ratio of 1:1 (v/v) and co-inoculated as a mixture of 20 µl (10^4 spore-cells of each) on the designated *Pseudonocardia*-infused media with 5 replicates per pairing. We used 150 plates for the S8 experiment (including 100 control plates; 10 replicates per pairing) and 100 plates for the S2 experiment (including 50 control plates; 5 replicates per pairing). Plates were incubated at 30 °C for 5 days before imaging, after which images were scored with respect to the producer as: win (dominant growth), draw (both strains growing with no clear dominant) or lose (little or no visible growth), always with reference to images of each strain grown alone on control medium to minimise observer bias. One plate's outcome was too ambiguous to score and was discarded. All plates were independently scored by two observers, one using photos of the original images, which produced datasets giving the same statistical results. We report the direct observer's scores. For analysis, draw outcomes were omitted, and a general linear mixed-effects model, including non-antibiotic-producer strain as a random intercept (10 groups), was used to test for an effect of the medium term (Control vs. Ps1/2-infused) on competitive outcome (Win vs. Loss) ((*lme4::glmer*(outcome ~ medium + (1 | non.producer.strain), family = binomial)). Significance was estimated using term deletion.

Antibiotic resistance assays. The key assumption of screening theory is that antibiotic-producers are better at resisting antibiotics, as measured by growth rates in the presence of antibiotics, because this correlation is what allows producer strains to better endure the demanding environment produced by *Pseudonocardia*. We tested this assumption by growing the 10 environmental producer strains, the 10 environmental non-producer strains, and the 10 resident non-producers strains (Additional File 1: Table S1) in the presence of 8 different antibiotics (Additional File 1: Table S4), representing a range of chemical classes and modes of action. Antibiotics were added to 1 ml of LB-Lennox/SFM medium (Additional File 1: Table S4) in a 24-well microtitre plate at 6 different concentrations. The relative concentration range was the same for each antibiotic, although actual concentrations reflected activity (Additional File 1: Table S4). Producers and non-producers were inoculated onto plates and incubated at 30 °C for 7 days, then photographed. Lowest Effective Concentration (LEC, lowest concentration with inhibitory effect) and Minimum Inhibitory Concentration (MIC, lowest concentration with no growth) scores were assigned on a Likert scale of 1–6, where 1 was no resistance and 6 was resistance above the concentrations tested (adapted from generalized MIC methods; reviewed by Balouiri *et al.*[65]).

Statistical analyses R markdown-format scripts, input datafiles, and html output files for the analyses in Main Text Figures 4, 5, and 6, and in Figures S9 & S10 (Additional File 1) are provided as a single R project folder at github.com/dougwyu/Worsley_et_al_screening_test_R_code [101]

Declarations

Ethics approval and consent to participate

Not applicable

Consent for publication

Not applicable

Availability of data and materials

The 16S rRNA gene amplicon sequencing data from the SIP experiment, as well as the RNA sequencing data have been uploaded to the European Nucleotide Archive (ENA), under the

accession numbers PRJEB32900 [90] and PRJEB32903 [92], respectively. R markdown-format scripts, input datafiles, and html output files for the analyses in Main Text Figures 4, 5, and 6, and in Additional file 1: Fig. S8 & S9 are also provided as a single R project folder at github.com/dougwyu/Worsley_et_al_screening_test_R_code [101].

Competing interests

The authors declare that they have no competing interests.

Funding

This work was supported by a NERC PhD studentship to SFW (NERC Doctoral Training Programme grant NE/L002582/1), NERC grants NE/J01074X/1 to MIH and DWY, NE/M015033/1 and NE/M014657/1 to MIH, JCM, DWY, and BW, European Research Council Advanced grant 323085 to JJB, and Marie Curie Individual European Fellowship grant 627949 to TI. DWY was also supported by the Key Research Program of Frontier Sciences, Chinese Academy of Sciences (QYZDY-SSW-SMC024) and the Strategic Priority Research Program, Chinese Academy of Sciences (XDA20050202, XDB31000000).

Authors' contributions

SFW, TMI, NAH, MMA-B, MS, BW, JCM, JJB, DWY and MIH designed the research. SFW, TI, NAH, JJB, DWY and MIH wrote the manuscript with comments from all other authors. SFW performed the RNA sequencing and RNA stable isotope probing experiments and maintained the captive ant colonies at UEA. TI, NAH, MMAB and MS cultured bacteria from the ants and performed the *in vitro* bioassays. SFW and DWY performed the statistical analysis. All authors read and approved the final manuscript.

Acknowledgements

We thank the Smithsonian Tropical Research Institute for logistical help and facilities for all work in Gamboa, Panama, and the Autoridad Nacional del Ambiente y el Mar for permission to sample and export ants to Copenhagen. We thank Simon Moxon for advice on RNA sequencing analysis; Paul Disdle for his assistentance with IRMS analysis; Elaine Patrick and Sylvia Matthiesen for lab and logistics support.

References

1. McCutcheon JP, Boyd BM, Dale C. The Life of an Insect Endosymbiont from the Cradle to the Grave. Curr Biol. 2019;29(11):R485-R95.

2. Brucker RM, Bordenstein SR. The hologenomic basis of speciation: gut bacteria cause hybrid lethality in the genus *Nasonia*. Science. 2013;341(6146):667-9.

3. Andersen SB, Yek SH, Nash DR, Boomsma JJ. Interaction specificity between leaf-cutting ants and vertically transmitted *Pseudonocardia* bacteria. BMC Evol Biol. 2015;15(1):1.

4. Kaltenpoth M, Göttler W, Herzner G, Strohm E. Symbiotic bacteria protect wasp larvae from fungal infestation. Curr Biol. 2005;15(5):475-9.

5. Engel P, Moran NA. The gut microbiota of insects - diversity in structure and function. FEMS Microbiol Rev. 2013;37(5):699-735.

6. Brune A. Symbiotic digestion of lignocellulose in termite guts. Nat Rev Microbiol. 2014;12(3):168-80.

7. Granato ET, Meiller-Legrand TA, Foster KR. The Evolution and Ecology of Bacterial Warfare. Curr Biol. 2019;29(11):R521-R37.

8. Foster KR, Schluter J, Coyte KZ, Rakoff-Nahoum S. The evolution of the host microbiome as an ecosystem on a leash. Nature. 2017;548(7665):43-51.

9. Widder S, Allen RJ, Pfeiffer T, Curtis TP, Wiuf C, Sloan WT, et al. Challenges in microbial ecology: building predictive understanding of community function and dynamics. ISME J. 2016;10(11):2557-68.

10. Hoye BJ, Fenton A. Animal host-microbe interactions. J Anim Ecol. 2018;87(2):315-9.

11. Archetti M, Ubeda F, Fudenberg D, Green J, Pierce NE, Yu DW. Let the right one in: a microeconomic approach to partner choice in mutualisms. Am Nat. 2011;177(1):75-85.

12. Scheuring I, Yu DW. How to assemble a beneficial microbiome in three easy steps. Ecol Lett. 2012;15(11):1300-7.

13. Boza G, Worsley SF, Yu DW, Scheuring I. Efficient assembly and long-term stability of defensive microbiomes via private resources and community bistability. Plos Comput Biol. 2019;15(5):e1007109.

14. Heil M. Let the best one stay: screening of ant defenders by *Acacia* host plants functions independently of partner choice or host sanctions. J Ecol. 2013;101(3):684-8.

15. Tragust S, Herrmann C, Häfner J, Braasch R, Tilgen C, Hoock M, et al. Formicine ants swallow their highly acidic poison for gut microbial selection and control. eLife. 2020;9:e60287.

16. Itoh H, Jang S, Takeshita K, Ohbayashi T, Ohnishi N, Meng XY, et al. Host-symbiont specificity determined by microbe-microbe competition in an insect gut. Proc Natl Acad Sci U S A. 2019;116(45):22673-82.

17. Ranger CM, Biedermann PHW, Phuntumart V, Beligala GU, Ghosh S, Palmquist DE, et al. Symbiont selection via alcohol benefits fungus farming by ambrosia beetles. Proc Natl Acad Sci U S A. 2018;115(17):4447-52.

18. Andersen SB, Hansen LH, Sapountzis P, Sorensen SJ, Boomsma JJ. Specificity and stability of the *Acromyrmex-Pseudonocardia* symbiosis. Mol Ecol. 2013;22(16):4307-21.

19. Chapela IH, Rehner SA, Schultz TR, Mueller UG. Evolutionary History of the Symbiosis Between Fungus-Growing Ants and Their Fungi. Science. 1994;266(5191):1691.

20. Mueller UG, Rehner SA, Schultz TR. The evolution of agriculture in ants. Science. 1998;281(5385):2034-8.

21. Currie CR. A community of ants, fungi, and bacteria: a multilateral approach to studying symbiosis. Annu Rev Microbiol. 2001;55(1):357-80.

22. De Fine Licht HH, Boomsma JJ, Tunlid A. Symbiotic adaptations in the fungal cultivar of leaf-cutting ants. Nat Commun. 2014;5:5675.

23. Sapountzis P, Zhukova M, Shik JZ, Schiott M, Boomsma JJ. Reconstructing the functions of endosymbiotic Mollicutes in fungus-growing ants. Elife. 2018;7.

24. Reynolds HT, Currie CR. Pathogenicity of *Escovopsis weberi*: The parasite of the attine ant-microbe symbiosis directly consumes the ant-cultivated fungus. Mycologia. 2004;96(5):955-9.

25. Heine D, Holmes NA, Worsley SF, Santos ACA, Innocent TM, Scherlach K, et al. Chemical warfare between leafcutter ant symbionts and a co-evolved pathogen. Nat Commun. 2018;9(1):2208.

26. Worsley SF, Innocent TM, Heine D, Murrell JC, Yu DW, Wilkinson B, et al. Symbiotic partnerships and their chemical interactions in the leafcutter ants (Hymenoptera: Formicidae). Myrmecol News. 2018;27:59-74.

27. de Man TJ, Stajich JE, Kubicek CP, Teiling C, Chenthamara K, Atanasova L, et al. Small genome of the fungus *Escovopsis weberi*, a specialized disease agent of ant agriculture. Proc Natl Acad Sci U S A. 2016;113(13):3567-72.

28. Currie CR, Stuart AE. Weeding and grooming of pathogens in agriculture by ants. Proc Biol Sci. 2001;268(1471):1033-9.

29. Fernandez-Marin H, Nash DR, Higginbotham S, Estrada C, van Zweden JS, d'Ettorre P, et al. Functional role of phenylacetic acid from metapleural gland secretions in controlling fungal pathogens in evolutionarily derived leaf-cutting ants. Proc Biol Sci. 2015;282(1807):20150212.

30. Fernandez-Marin H, Zimmerman JK, Rehner SA, Wcislo WT. Active use of the metapleural glands by ants in controlling fungal infection. Proc Biol Sci. 2006;273(1594):1689-95.

31. Currie CR, Scott JA, Summerbell RC, Malloch D. Fungus-growing ants use antibiotic-producing bacteria to control garden parasites. Nature. 1999;398(6729):701-4.

32. Holmes NA, Innocent TM, Heine D, Bassam MA, Worsley SF, Trottmann F, et al. Genome analysis of two *Pseudonocardia* phylotypes associated with *Acromyrmex* leafcutter ants reveals their biosynthetic potential. Front Microbiol. 2016;7:2073.

33. Poulsen M, Cafaro M, Boomsma JJ, Currie CR. Specificity of the mutualistic association between actinomycete bacteria and two sympatric species of *Acromyrmex* leaf-cutting ants. Mol Ecol. 2005;14(11):3597-604.

34. Marsh SE, Poulsen M, Pinto-Tomás A, Currie CR. Interaction between workers during a short time window is required for bacterial symbiont transmission in *Acromyrmex* leaf-cutting ants. PLoS One. 2014;9(7):e103269.

35. Poulsen M, Bot ANM, Currie CR, Nielsen MG, Boomsma JJ. Within-colony transmission and the cost of a mutualistic bacterium in the leaf-cutting ant *Acromyrmex octospinosus*. Funct Ecol. 2003;17(2):260-9.

36. Kost C, Lakatos T, Böttcher I, Arendholz W-R, Redenbach M, Wirth R. Non-specific association between filamentous bacteria and fungus-growing ants. Naturwissenschaften. 2007;94(10):821-8.

37. Barke J, Seipke RF, Gruschow S, Heavens D, Drou N, Bibb MJ, et al. A mixed community of actinomycetes produce multiple antibiotics for the fungus farming ant *Acromyrmex octospinosus*. BMC Biol. 2010;8.

38. Haeder S, Wirth R, Herz H, Spiteller D. Candicidin-producing *Streptomyces* support leaf-cutting ants to protect their fungus garden against the pathogenic fungus *Escovopsis*. Proc Natl Acad Sci USA. 2009;106(12):4742-6.

39. Schoenian I, Spiteller M, Ghaste M, Wirth R, Herz H, Spiteller D. Chemical basis of the synergism and antagonism in microbial communities in the nests of leaf-cutting ants. Proc Natl Acad Sci U S A. 2011;108(5):1955-60.

40. Sen R, Ishak HD, Estrada D, Dowd SE, Hong E, Mueller UG. Generalized antifungal activity and 454-screening of *Pseudonocardia* and *Amycolatopsis* bacteria in nests of fungus-growing ants. Proc Natl Acad Sci USA. 2009;106(42):17805.

41. Currie CR, Poulsen M, Mendenhall J, Boomsma JJ, Billen J. Coevolved crypts and exocrine glands support mutualistic bacteria in fungus-growing ants. Science. 2006;311(5757):81-3.

42. Dumont MG, Murrell JC. Stable isotope probing - linking microbial identity to function. Nat Rev Microbiol. 2005;3(6):499-504.

43. Neufeld JD, Wagner M, Murrell JC. Who eats what, where and when? Isotope-labelling experiments are coming of age. ISME J. 2007;1(2):103-10.

44. Whiteley AS, Thomson B, Lueders T, Manefield M. RNA stable-isotope probing. Nat Protoc. 2007;2(4):838-44.

45. Andersen SB, Boye M, Nash DR, Boomsma JJ. Dynamic *Wolbachia* prevalence in *Acromyrmex* leaf-cutting ants: potential for a nutritional symbiosis. J Evol Biol. 2012;25(7):1340-50.

46. Sapountzis P, Nash DR, Schiott M, Boomsma JJ. The evolution of abdominal microbiomes in fungus-growing ants. Mol Ecol. 2019;28(4):879-99.

47. Seipke RF, Barke J, Brearley C, Hill L, Douglas WY, Goss RJ, et al. A single *Streptomyces* symbiont makes multiple antifungals to support the fungus farming ant *Acromyrmex octospinosus*. PLoS One. 2011;6(8):e22028.

48. Gomez-Escribano JP, Bibb MJ. Engineering *Streptomyces coelicolor* for heterologous expression of secondary metabolite gene clusters. Microb Biotechnol. 2011;4(2):207-15.

49. Hopwood DA, Kieser T, Wright HM, Bibb MJ. Plasmids, Recombination and Chromosome Mapping in *Streptomyces lividans* 66. Microbiology. 1983;129(7):2257-69.

50. Bentley SD, Chater KF, Cerdeno-Tarraga AM, Challis GL, Thomson NR, James KD, et al. Complete genome sequence of the model actinomycete *Streptomyces coelicolor* A3(2). Nature. 2002;417(6885):141-7.

51. Bignell DR, Seipke RF, Huguet-Tapia JC, Chambers AH, Parry RJ, Loria R. *Streptomyces scabies* 87-22 contains a coronafacic acid-like biosynthetic cluster that contributes to plant-microbe interactions. Mol Plant Microbe Interact. 2010;23(2):161-75.

52. Seipke RF, Barke J, Heavens D, Yu DW, Hutchings MI. Analysis of the bacterial communities associated with two ant-plant symbioses. Microbiologyopen. 2013;2(2):276-83.

53. Holmes NA, Devine R, Qin Z, Seipke RF, Wilkinson B, Hutchings MI. Complete genome sequence of *Streptomyces formicae* KY5, the formicamycin producer. J Biotechnol. 2018;265:116-8.

54. Seipke RF, Patrick E, Hutchings MI. Regulation of antimycin biosynthesis by the orphan ECF RNA polymerase sigma factor sigma (AntA.). PeerJ. 2014;2:e253.

55. Nygaard S, Zhang G, Schiott M, Li C, Wurm Y, Hu H, et al. The genome of the leaf-cutting ant *Acromyrmex echinatior* suggests key adaptations to advanced social life and fungus farming. Genome Res. 2011;21(8):1339-48.

56. Muyzer G, de Waal EC, Uitterlinden AG. Profiling of complex microbial populations by denaturing gradient gel electrophoresis analysis of polymerase chain reaction-amplified genes coding for 16S rRNA. Appl Environ Microbiol. 1993;59(3):695-700.

57. Gershenzon J, Dudareva N. The function of terpene natural products in the natural world. Nat Chem Biol. 2007;3(7):408-14.

58. Richter TK, Hughes CC, Moore BS. Sioxanthin, a novel glycosylated carotenoid, reveals an unusual subclustered biosynthetic pathway. Environ Microbiol. 2015;17(6):2158-71.

59. Nupur LN, Vats A, Dhanda SK, Raghava GP, Pinnaka AK, Kumar A. ProCarDB: a database of bacterial carotenoids. BMC Microbiol. 2016;16:96.

60. Chikindas ML, Weeks R, Drider D, Chistyakov VA, Dicks LM. Functions and emerging applications of bacteriocins. Curr Opin Biotechnol. 2018;49:23-8.

61. Cotter PD, Ross RP, Hill C. Bacteriocins - a viable alternative to antibiotics? Nat Rev Microbiol. 2013;11(2):95-105.

62. Riley MA, Gordon DM. The ecological role of bacteriocins in bacterial competition. Trends Microbiol. 1999;7(3):129-33.

63. Algburi A, Zehm S, Netrebov V, Bren AB, Chistyakov V, Chikindas ML. Subtilosin Prevents Biofilm Formation by Inhibiting Bacterial Quorum Sensing. Probiotics Antimicrob Proteins. 2017;9(1):81-90.

64. Bates D, Mächler M, Bolker B, Walker S. Fitting Linear Mixed-Effects Models Using lme4. J Stat Softw. 2015;1(1).

65. Balouiri M, Sadiki M, Ibnsouda SK. Methods for *in vitro* evaluating antimicrobial activity: A review. J Pharm Anal. 2016;6(2):71-9.

66. Currie C, Bot A, Boomsma JJ. Experimental evidence of a tripartite mutualism: bacteria protect ant fungus gardens from specialized parasites. Oikos. 2003;101(1):91-102.

67. Oldroyd GE. Speak, friend, and enter: signalling systems that promote beneficial symbiotic associations in plants. Nat Rev Microbiol. 2013;11(4):252-63.

68. Archetti M, Miller JB, Yu DW. Evolution of passwords for cost-free honest signalling between symbionts and hosts. bioRxiv. 2016:065755.

69. McLaren MR, Willis AD, Callahan BJ. Consistent and correctable bias in metagenomic sequencing experiments. Elife. 2019;8.

70. Williamson BD, Hughes JP, Willis AD. A multiview model for relative and absolute microbial abundances. Biometrics. 2021.

71. Poulsen M, Bot AN, Boomsma JJ. The effect of metapleural gland secretion on the growth of a mutualistic bacterium on the cuticle of leaf-cutting ants. Naturwissenschaften. 2003;90(9):406-9.

72. Musat N, Musat F, Weber PK, Pett-Ridge J. Tracking microbial interactions with NanoSIMS. Curr Opin Biotechnol. 2016;41:114-21.

73. Berry D, Stecher B, Schintlmeister A, Reichert J, Brugiroux S, Wild B, et al. Host-compound foraging by intestinal microbiota revealed by single-cell stable isotope probing. Proc Natl Acad Sci U S A. 2013;110(12):4720-5.

74. Wang Y, Huang WE, Cui L, Wagner M. Single cell stable isotope probing in microbiology using Raman microspectroscopy. Curr Opin Biotechnol. 2016;41:34-42.

75. Haeder S, Wirth R, Herz H, Spiteller D. Candicidin-producing *Streptomyces* support leaf-cutting ants to protect their fungus garden against the pathogenic fungus *Escovopsis*. Proc Natl Acad Sci. 2009;106(12):4742-6.

76. Bertrand S, Bohni N, Schnee S, Schumpp O, Gindro K, Wolfender JL. Metabolite induction via microorganism co-culture: a potential way to enhance chemical diversity for drug discovery. Biotechnol Adv. 2014;32(6):1180-204.

77. Lee N, Kim W, Chung J, Lee Y, Cho S, Jang KS, et al. Iron competition triggers antibiotic biosynthesis in *Streptomyces coelicolor* during coculture with Myxococcus xanthus. ISME J. 2020;14(5):1111-24.

78. Zivkovic AM, German JB, Lebrilla CB, Mills DA. Human milk glycobiome and its impact on the infant gastrointestinal microbiota. Proc Natl Acad Sci U S A. 2011;108 Suppl 1:4653-8.

79. Brinker P, Weig A, Rambold G, Feldhaar H, Tragust S. Microbial community composition of nest-carton and adjoining soil of the ant Lasius fuliginosus and the role of host secretions in structuring microbial communities. Fungal Ecol. 2019;38:44-53.

80. Carlstrom CI, Field CM, Bortfeld-Miller M, Muller B, Sunagawa S, Vorholt JA. Synthetic microbiota reveal priority effects and keystone strains in the *Arabidopsis* phyllosphere. Nat Ecol Evol. 2019;3(10):1445-54.

81. Cai T, Cai W, Zhang J, Zheng H, Tsou AM, Xiao L, et al. Host legume-exuded antimetabolites optimize the symbiotic rhizosphere. Mol Microbiol. 2009;73(3):507-17.

82. Neal AL, Ahmad S, Gordon-Weeks R, Ton J. Benzoxazinoids in root exudates of maize attract *Pseudomonas putida* to the rhizosphere. PLoS One. 2012;7(4):e35498.

83. Wippel K, Tao K, Niu Y, Zgadzaj R, Kiel N, Guan R, et al. Host preference and invasiveness of commensal bacteria in the Lotus and Arabidopsis root microbiota. Nat Microbiol. 2021.

84. Ryan PR, Dessaux Y, Thomashow LS, Weller DM. Rhizosphere engineering and management for sustainable agriculture. Plant and Soil. 2009;321(1):363-83.

85. Lueders T, Manefield M, Friedrich MW. Enhanced sensitivity of DNA- and rRNA-based stable isotope probing by fractionation and quantitative analysis of isopycnic centrifugation gradients. Environ Microbiol. 2004;6(1):73-8.

86. Dowd SE, Callaway TR, Wolcott RD, Sun Y, McKeehan T, Hagevoort RG, et al. Evaluation of the bacterial diversity in the feces of cattle using 16S rDNA bacterial tag-encoded FLX amplicon pyrosequencing (bTEFAP). BMC Microbiol. 2008;8:125.

87. Dowd SE, Wolcott RD, Sun Y, McKeehan T, Smith E, Rhoads D. Polymicrobial nature of chronic diabetic foot ulcer biofilm infections determined using bacterial tag encoded FLX amplicon pyrosequencing (bTEFAP). PLoS One. 2008;3(10):e3326.

88. DeSantis TZ, Hugenholtz P, Larsen N, Rojas M, Brodie EL, Keller K, et al. Greengenes, a chimera-checked 16S rRNA gene database and workbench compatible with ARB. Appl Environ Microbiol. 2006;72(7):5069-72.

89. R Core Team. R: A language and environment for statistical computing. R Foundation for Statistical Computing, Vienna, Austria. https://www.R-project.org/. 2017.

90. PRJEB32900- RNA stable isotope probing in *A. echinatior* ants. European Nucleotide Archive. https://www.ebi.ac.uk/ena/browser/view/PRJEB32900. 2019.

91. Westermann AJ, Forstner KU, Amman F, Barquist L, Chao Y, Schulte LN, et al. Dual RNA-seq unveils noncoding RNA functions in host-pathogen interactions. Nature. 2016;529(7587):496-501.

92. PRJEB32903- Dual RNA sequencing of A. echinatior leafcutter ant laterocervical plates to establish secondary metabolite production by Pseudonocardia symbionts in vivo. https://www.ebi.ac.uk/ena/browser/view/PRJEB32903. 2019.

93. Kim D, Langmead B, Salzberg SL. HISAT: a fast spliced aligner with low memory requirements. Nat Methods. 2015;12(4):357-60.

94. Anders S, Pyl PT, Huber W. HTSeq- a Python framework to work with high-throughput sequencing data. Bioinformatics. 2015;31(2):166-9.

95. Mortazavi A, Williams BA, McCue K, Schaeffer L, Wold B. Mapping and quantifying mammalian transcriptomes by RNA-Seq. Nat Methods. 2008;5(7):621-8.

96. Kanehisa M, Sato Y, Morishima K. BlastKOALA and GhostKOALA: KEGG tools for functional characterization of genome and metagenome sequences. J Mol Biol. 2016;428(4):726-31.

97. Blin K, Wolf T, Chevrette MG, Lu X, Schwalen CJ, Kautsar SA, et al. antiSMASH 4.0-improvements in chemistry prediction and gene cluster boundary identification. Nucleic Acids Res. 2017;45(W1):W36-W41.

98. Kieser T, Bibb MJ, Buttner MJ, Chater KF, Hopwood DA. Practical *Streptomyces* Genetics. Norwich: John Innes Foundation; 2000.

99. Rueden CT, Schindelin J, Hiner MC, DeZonia BE, Walter AE, Arena ET, et al. ImageJ2: ImageJ for the next generation of scientific image data. BMC Bioinformatics. 2017;18(1):529.

100. Schindelin J, Arganda-Carreras I, Frise E, Kaynig V, Longair M, Pietzsch T, et al. Fiji: an open-source platform for biological-image analysis. Nat Methods. 2012;9(7):676-82.

101. Worsley SF, Innocent TM, Holmes NA, M. A-BM, Wilkinson B, Murrell JC, et al. Competition-based screening secures the evolutionary stability of a defensive

microbiome. GitHub Repository. https://github.com/dougwyu/Worsley_et_al_screening_test_R_code. 2021.

Figure Legends

Figure 1. Frequencies of bacteria at different taxonomic levels in unfractionated RNA samples from the propleural plates of ants provided with a 20% (w/v) solution of either ^{12}C- or ^{13}C-labelled glucose. (**A**) Phylum resolution, showing that >75% were actinobacteria. The remaining reads almost all corresponded to *Wolbachia* (Proteobacteria) so the three other phyla do not appear in the bars (total relative abundance of 0.6% and 0.4% in ^{12}C and ^{13}C fractions, respectively). As *Wolbachia* is not part of the cuticular microbiome (see text), these results show that the cuticular microbiome is completely dominated by actinobacteria. (**B**) Genus-level resolution showing that the cuticular microbiomes are dominated by the native *Pseudonocardia* symbiont followed by appreciable fractions of horizontally acquired *Streptomyces* species and a series of other actinobacteria at low prevalence.

Figure 2. Normalised abundances of the genera *Pseudonocardia* (**A**), *Streptomyces* (**B**), *Microbacterium* (**C**), and *Wolbachia* (**D**) in buoyant density fractions of RNA samples taken from ants fed on a ^{13}C (black) or ^{12}C (grey) glucose diet. There were three replicate samples per treatment. The relative abundances of genera were normalised by multiplying by the percentage of 16S rRNA gene transcripts occurring in each fraction within a sample (see Additional file 1: Fig. S4).

Figure 3. Expression (in reads per kilobase of transcript per million mapped reads, RPKM) of (**A**) biosynthetic gene clusters that are shared between the two *Pseudonocardia* species, (**B**) biosynthetic gene clusters that are unique to *P. octospinosus* (colony Ae1083) and (**C**) biosynthetic gene clusters that are unique to *P. echinatior* (colony Ae088). Biosynthetic gene cluster codes relate to Additional File 1: Table S3. Results from each colony were derived from a pool of 80 ants.

Figure 4. Growth-rate experiments. Bacterial colony sizes after 5 days at 30 ºC. Boxplots indicate medians ± one quartile. The white section shows growth rates on control media, and the coloured section shows growth rates on the *Pseudonocardia*-infused media. Red boxes

represent non-antibiotic-producer strains, and blue boxes represent antibiotic-producing *Streptomyces* strains. A linear mixed-effects model [64], including 17 *Pseudonocardia* strains and 20 inoculated bacterial species as random intercepts, was used to test for interaction and main effects of growth media (Control vs. Ps1.infused vs. Ps2.infused) and antibiotic production (Non.producers vs. Producers): *lme4::lmer*(Growth.score ~ Growth.media * Antibiotic.production + (1|Ps.strain/Plate)+(1|In.strain)). One non-producer strain (*Staphylococcus epidermidis*) grew more rapidly than all other strains (open triangle points), demonstrating the need to control for correlated residuals.

Figure 5. Antibiotic resistance profiles (**A** LEC and **B** MIC) for producers and non-producer strains (Additional file 1: Table S1), based upon each strain's mean growth score across the eight tested antibiotics (details in Additional file 1: Table S4). Boxplots indicate medians (notches) ± one quartile. 'Rabbit ears' in **B** indicate that the medians are also the highest values.

Figure 6. Pairwise competition experiment, scoring the frequency of producer wins. (**A**) Representative images of agar plates at five days post-inoculation showing examples of the three competitive outcomes: Win (producer S2 vs. non-producer St3 on Ps2 media), Loss (producer S8 vs. non-producer St3 on control media), and Draw (producer S2 vs. non-producer St3 on control media) (strain details in Additional file 1: Table S1). (**B**) Bar charts of competitive outcomes for the two *Streptomyces* producer strains (S8 and S2; Additional file 1: Table S1). Each *Streptomyces* strain was individually competed against ten different non-antibiotic-producer strains. *Streptomyces* is more likely to win on *Pseudonocardia*-infused media. A general linear mixed-effects model, with ten non-antibiotic-producer strains as a random intercept, was used to test for effect of medium (Control vs. Ps-infused) on competitive outcome (Win vs. Loss). For analysis, draws were omitted. S8 on Ps1-infused media: $n_{Ps1\text{-}infused}=34$, $n_{Control}=95$, $\chi^2 = 103.6$, df = 1, $p < 0.0001$; S2 on Ps2-infused media: general linear mixed-effects model, $n_{Ps2\text{-}infused} =50$, $n_{Control}=44$, $\chi^2 = 87.9$, df = 1, $p < 0.0001$. *lme4::glmer*(outcome ~ medium + (1 | non.producer.strain), family = binomial).

Supplementary Information

Additional file 1.

A PDF (.pdf) file containing the following supplemental tables, figures and methods referenced in the text: **Fig. S1:** Overview of methodology used for RNA stable isotope probing; **Fig. S2.** Fluorescent microscopy images of glucose water diet treatment; **Fig. S3.** The relationship between RNA-SIP fraction number and buoyant density; **Fig. S4.** 16S rRNA gene copy number across different fractions of buoyant density gradients, as determined via qPCR; **Fig. S5.** The atom percentage of ^{13}C in ants, as determined by Isotope Ratio Mass Spectrometry (IRMS) analysis; **Fig. S6.** The expression of Kegg orthology pathway categories in *Pseudonocardia* symbiont strains; **Fig. S7.** The bioactivity of *Pseudonocardia* isolates against the specialized fungus-garden pathogen *Escovopsis weberi*; **Fig. S8**. Individual growth-rate experiments of *Acromyrmex*-resident, non-producer strains; **Fig. S9.** Antibiotic resistance profiles for producer, non-producer, and resident non-producer strains; **Table S1.** Details of ant colonies, bacterial and fungal strains, reference genomes and primers used in experiments; **Table S2.** Details RNA-sequencing reads from ant propleural plate samples; **Table S3.** Secondary metabolite BGCs in the *Pseudonocardia* mutualist genomes (table adapted from [32]); **Table S4**. Media recipes and antibiotics used in this study.

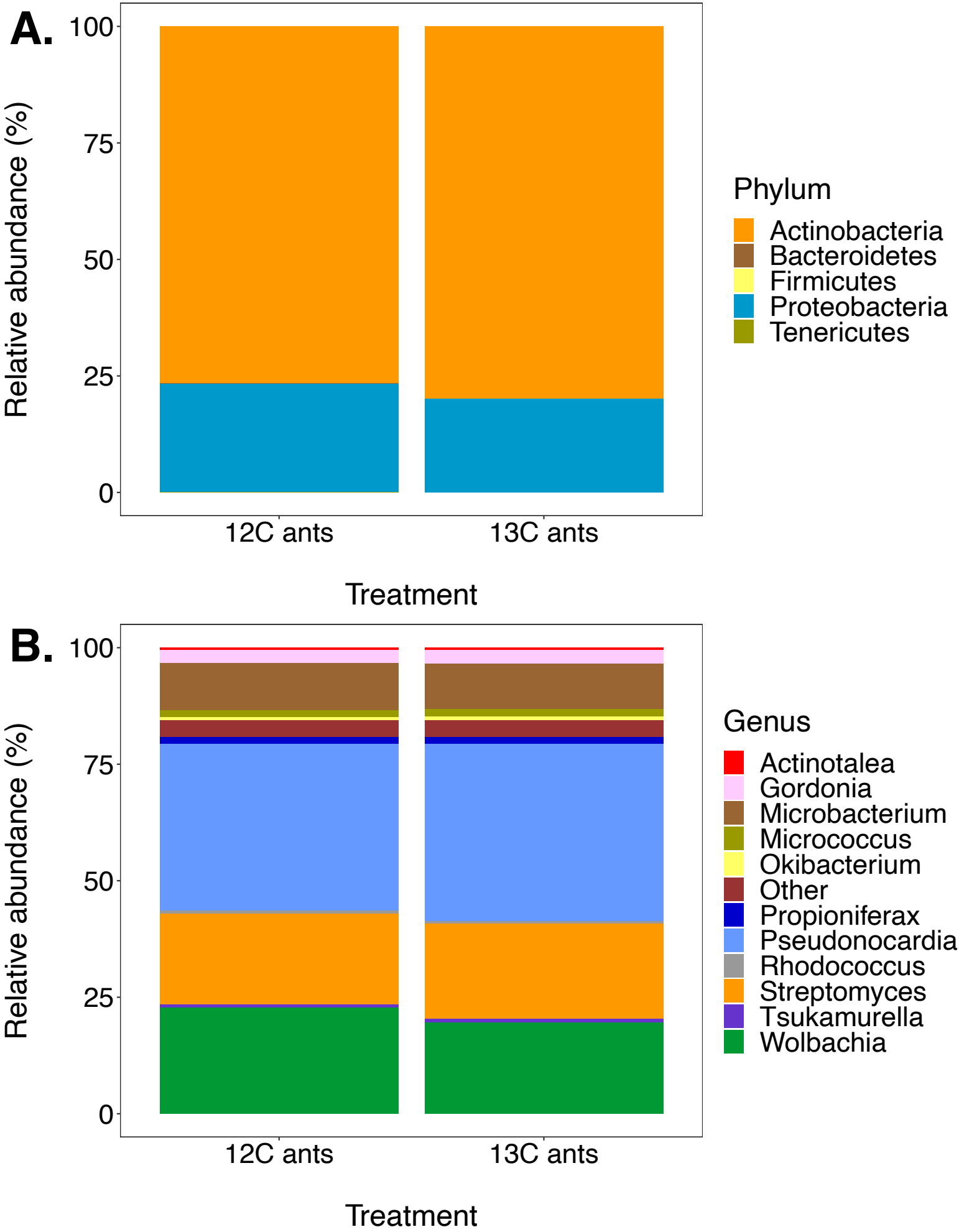
A.
100
75
50
25
0
Relative abundance (%)
12C ants
13C ants
Treatment
Phylum
Actinobacteria
Bacteroidetes
Firmicutes
Proteobacteria
Tenericutes
B.
100
75
50
25
0
Relative abundance (%)
12C ants
13C ants
Treatment
Genus
Actinotalea
Gordonia
Microbacterium
Micrococcus
Okibacterium
Other
Propioniferax
Pseudonocardia
Rhodococcus
Streptomyces
Tsukamurella
Wolbachia

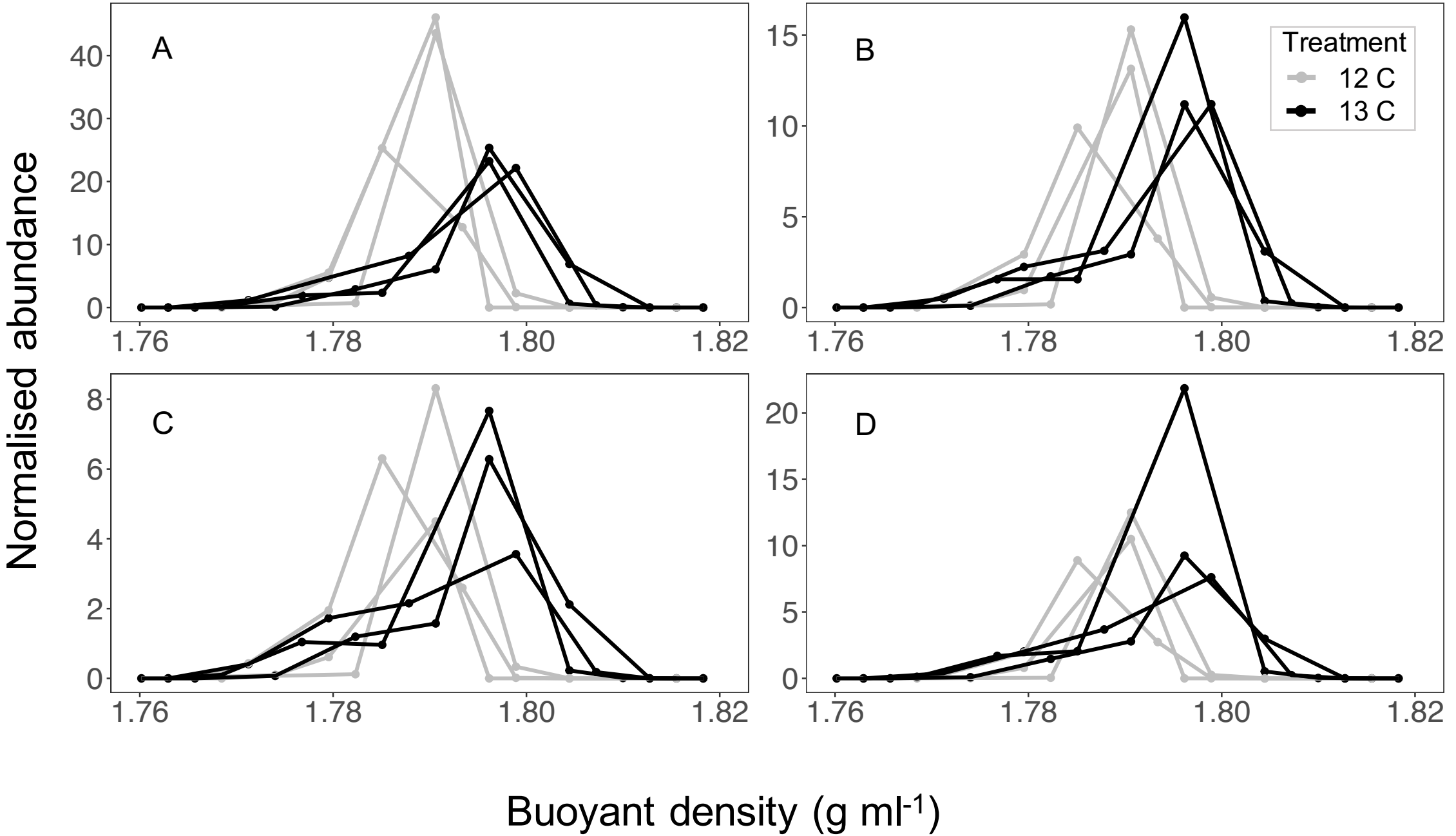
A
B
C
D
Treatment
12 C
13 C
Normalised abundance
Buoyant density (g ml-1)
1.76
1.78
1.80
1.82

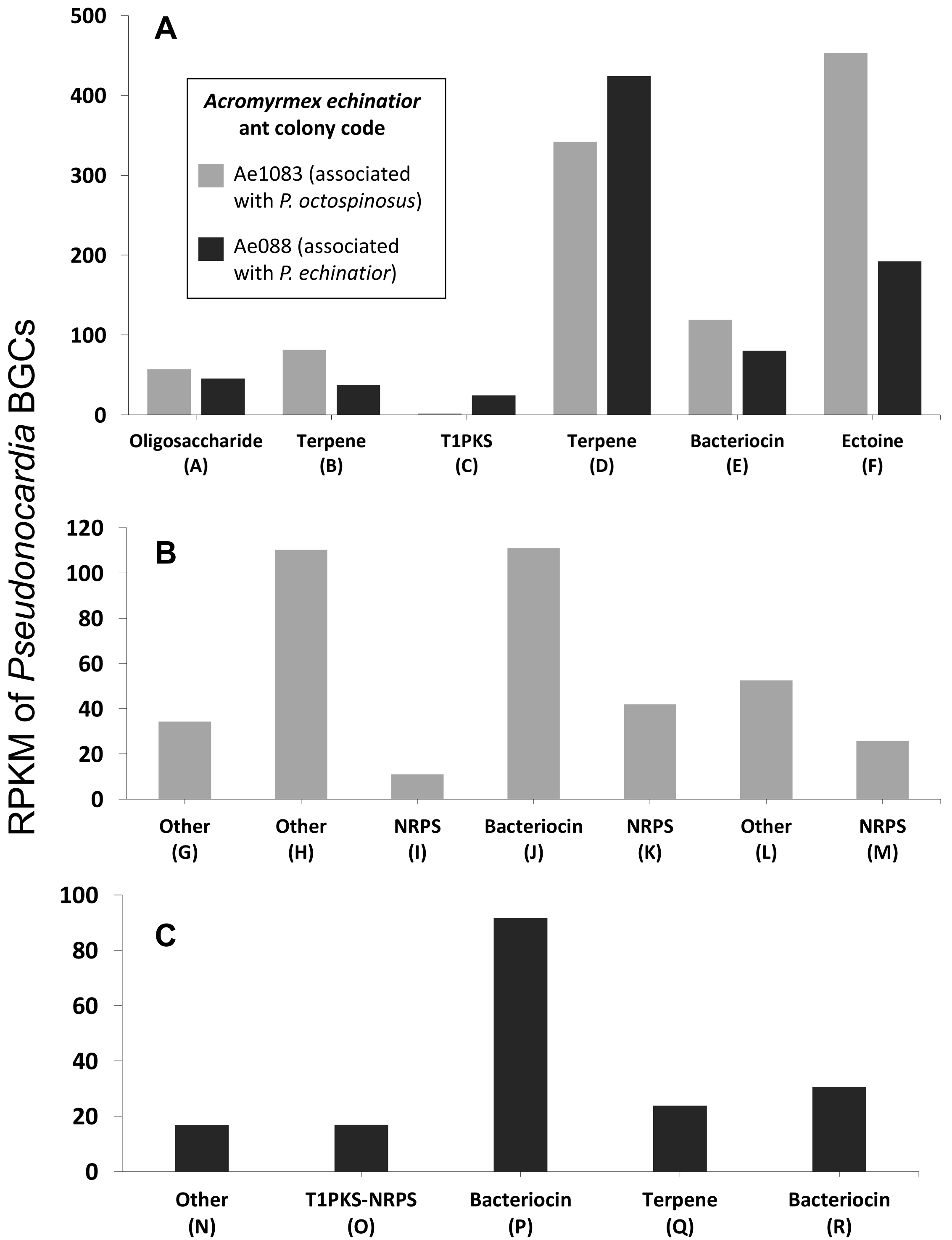
A
Acromyrmex echinatior ant colony code
Ae1083 (associated with P. octospinosus)
Ae088 (associated with P. echinatior)
500
400
300
200
100
0
Oligosaccharide (A)
Terpene (B)
T1PKS (C)
Terpene (D)
Bacteriocin (E)
Ectoine (F)
B
120
100
80
60
40
20
0
Other (G)
Other (H)
NRPS (I)
Bacteriocin (J)
NRPS (K)
Other (L)
NRPS (M)
C
100
80
60
40
20
0
Other (N)
T1PKS-NRPS (O)
Bacteriocin (P)
Terpene (Q)
Bacteriocin (R)
RPKM of Pseudonocardia BGCs

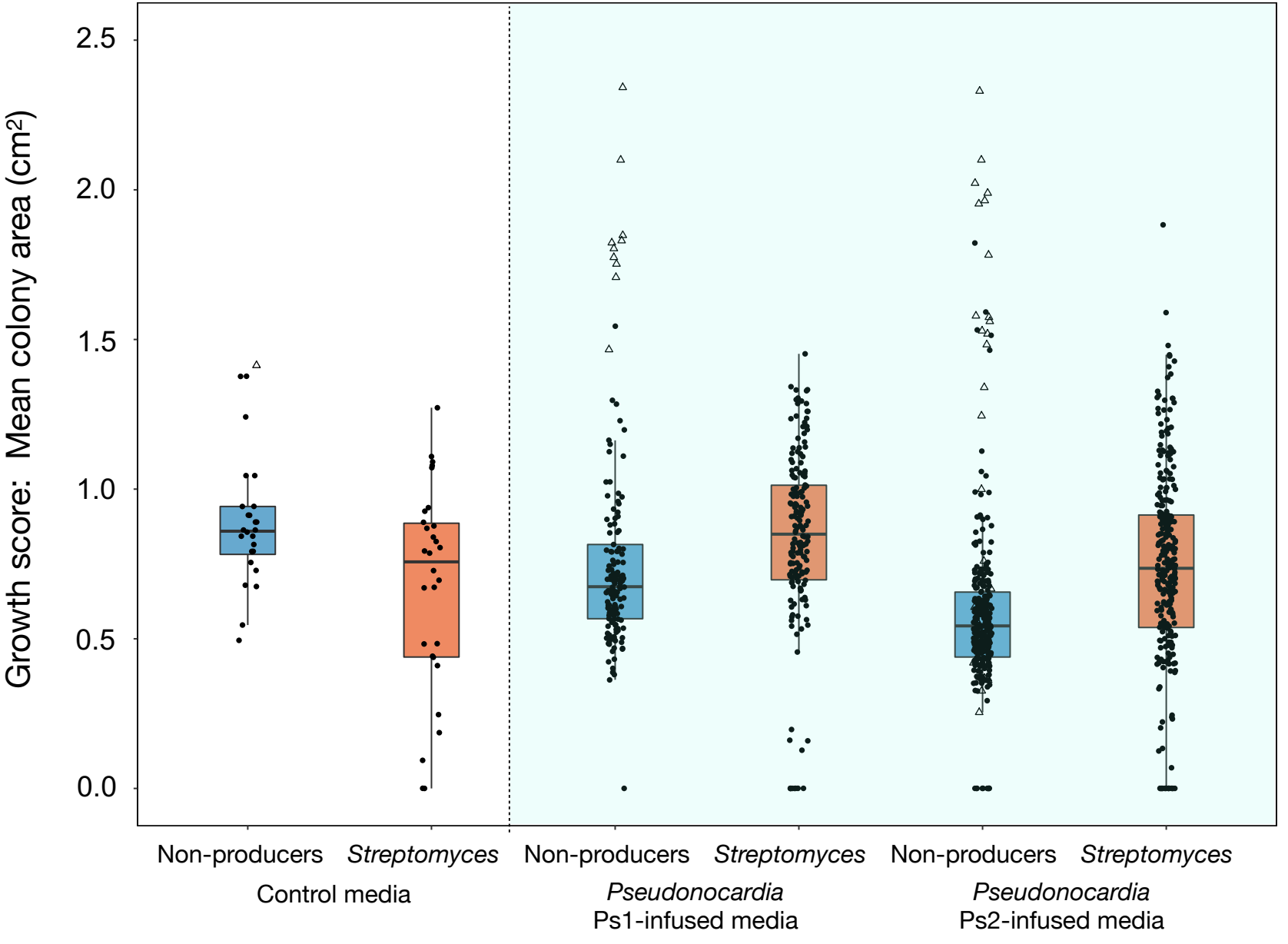
Growth score: Mean colony area (cm²)
2.5
2.0
1.5
1.0
0.5
0.0
Non-producers
Streptomyces
Control media
Non-producers
Streptomyces
Pseudonocardia
Ps1-infused media
Non-producers
Streptomyces
Pseudonocardia
Ps2-infused media

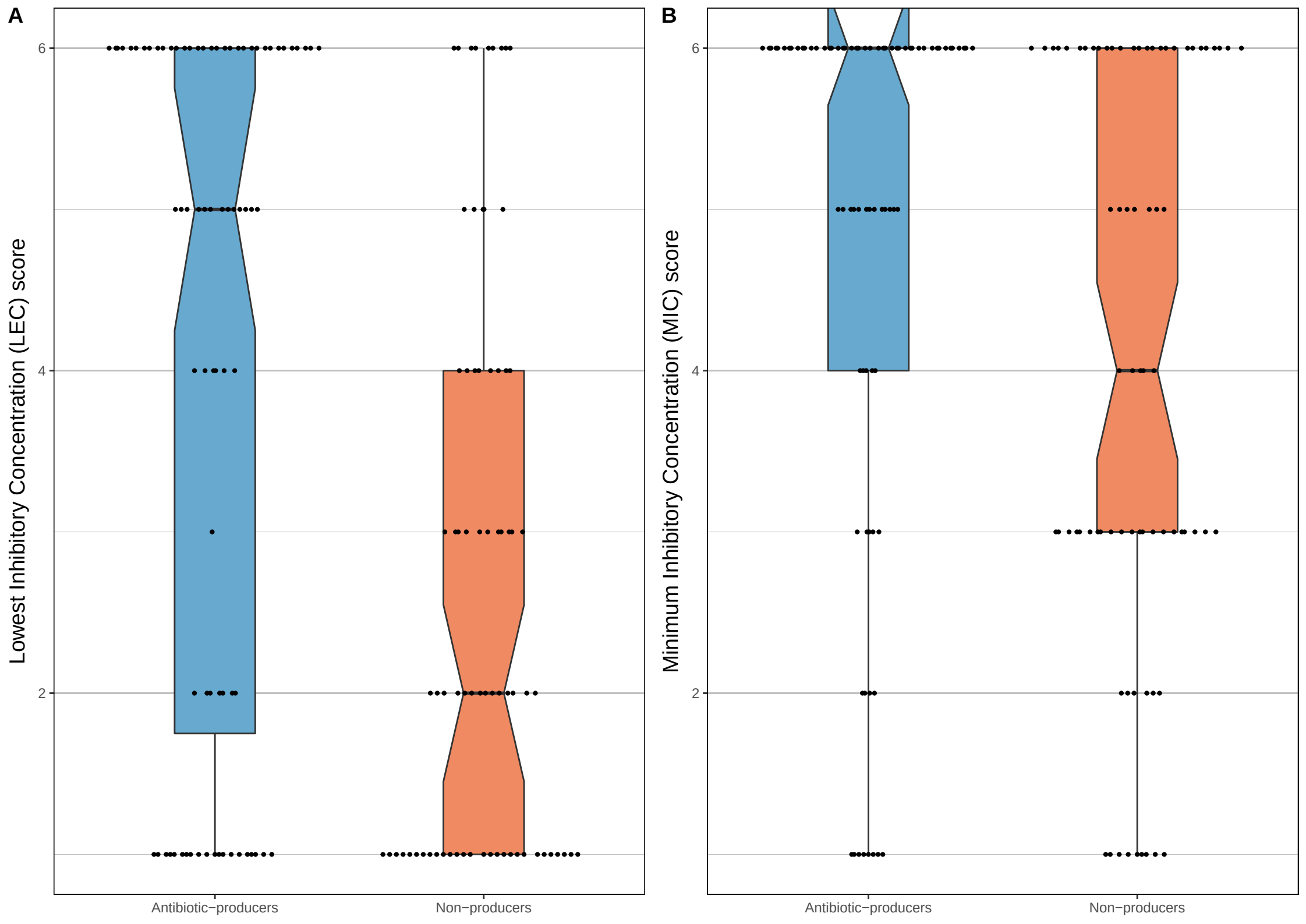
A
B
Lowest Inhibitory Concentration (LEC) score
Minimum Inhibitory Concentration (MIC) score
6
4
2
Antibiotic−producers
Non−producers

A

Streptomyces win | Draw | *Streptomyces* loss

B

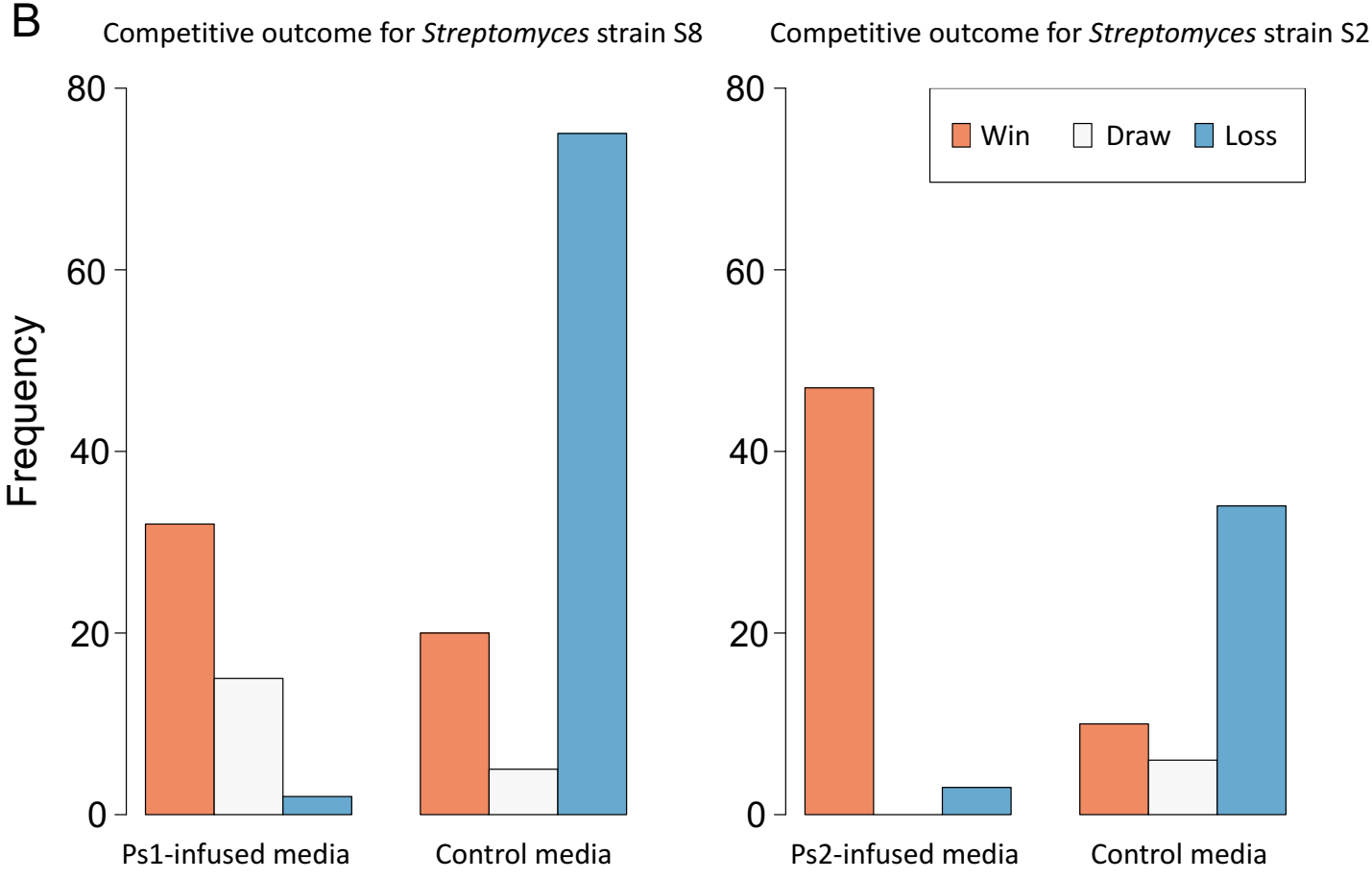

Competition-based screening helps to secure the evolutionary stability of a defensive microbiome: Additional file 1

Sarah F. Worsley[1], Tabitha M. Innocent[2,†], Neil A. Holmes[1,3,†], Mahmoud M. Al-Bassam[1], Morten Schiøtt[2], Barrie Wilkinson[3], J. Colin Murrell[4], Jacobus J. Boomsma[2*], Douglas W. Yu[1,5,6,*], Matthew I. Hutchings[1,3,*]

[1]School of Biological Sciences, University of East Anglia, Norwich Research Park, Norwich, Norfolk, UK, NR4 7TJ

[2]Centre for Social Evolution, Section for Ecology and Evolution, Department of Biology, University of Copenhagen, Copenhagen, Denmark.

[3]Department of Molecular Microbiology, John Innes Centre, Norwich Research Park, Norwich, Norfolk, UK, NR4 7UH

[4]School of Environmental Sciences, University of East Anglia, Norwich Research Park, Norwich, Norfolk, UK, NR4 7TJ

[5]State Key Laboratory of Genetic Resources and Evolution, Kunming Institute of Zoology, Chinese Academy of Sciences, Kunming, Yunnan, China 650223

[6]Center for Excellence in Animal Evolution and Genetics, Chinese Academy of Sciences, Kunming Yunnan, China 650223

†These authors contributed equally to the manuscript

*Correspondence: matt.hutchings@jic.ac.uk, jjboomsma@bio.ku.dk, douglas.yu@uea.ac.uk

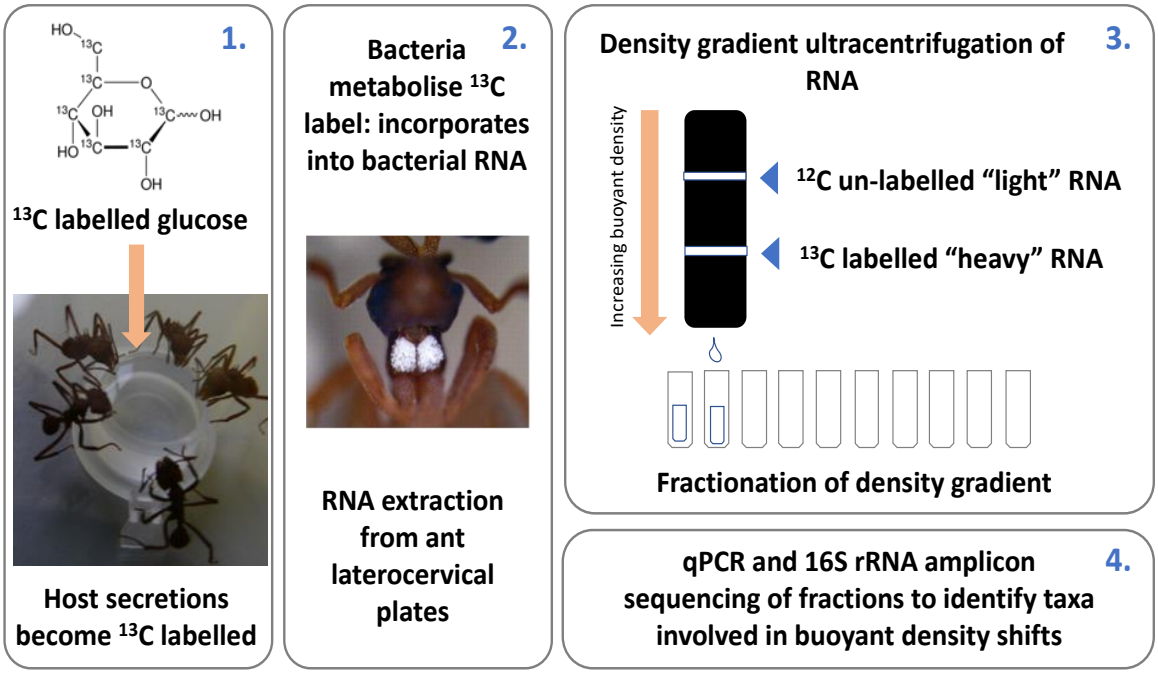

Figure S1. Overview of methodology used for RNA stable isotope probing of the propleural plate microbiome of *Acromyrmex echinatior* leaf-cutting ants.

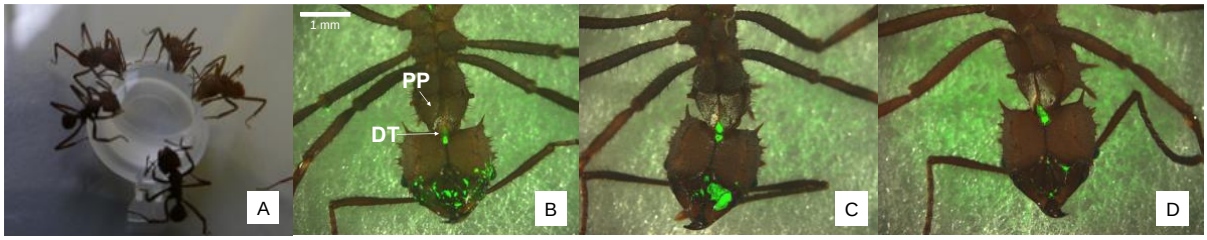

Figure S2. The extent to which a 20% (w/v) glucose water diet containing green fluorescent dye (A) was distributed over the ant body directly after taking a feed (B), 6 hours after feeding (C) and 24 hours after feeding (D). DT = fluorescence shining through from the ant digestive tract, PP = propleural plates with growth of actinobacteria.

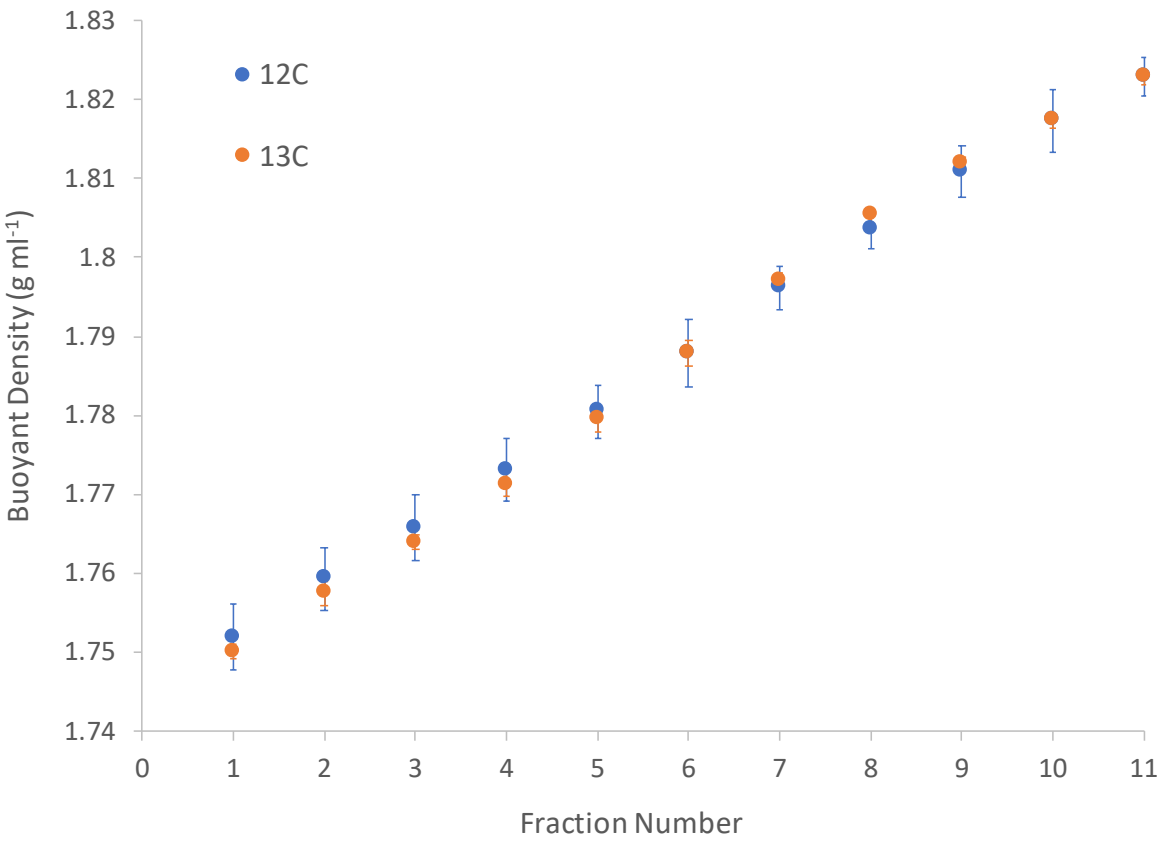

Figure S3. The relationship between RNA-SIP fraction number and buoyant density (in g ml^{-1}). Fractions were generated from density gradients containing RNA isolated from the propleural plates of *A. echinatior* ants fed on either a ^{12}C (blue) or a ^{13}C (orange) glucose water diet. Points represent averages (three samples each of 22 ants per dietary treatment) ± standard error.

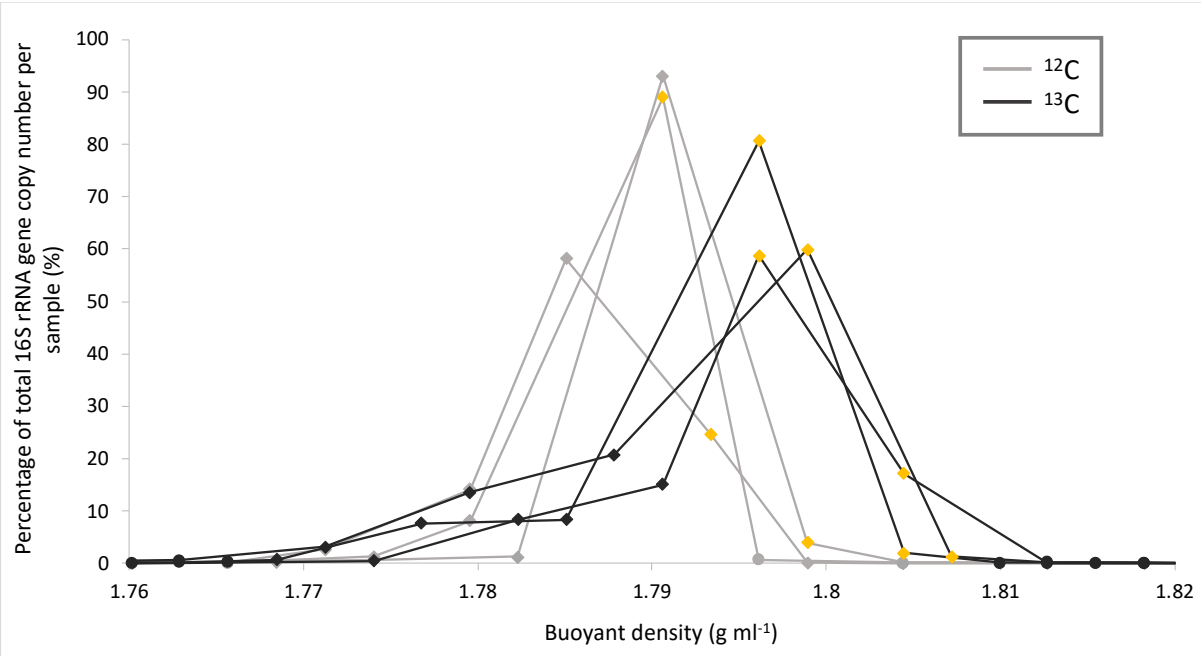

Figure S4. 16S rRNA gene copy number across different fractions of buoyant density gradients, as determined via qPCR. Gene copy number in each fraction is displayed as a percentage of total copy number in each sample. There were three replicate samples of 22 ants fed a ^{12}C (light grey) or ^{13}C (dark grey) glucose diet. Diamond symbols represent fractions that were sent for 16S rRNA gene amplicon sequencing and yellow diamonds represent those designated as "heavy" fractions under the different treatments.

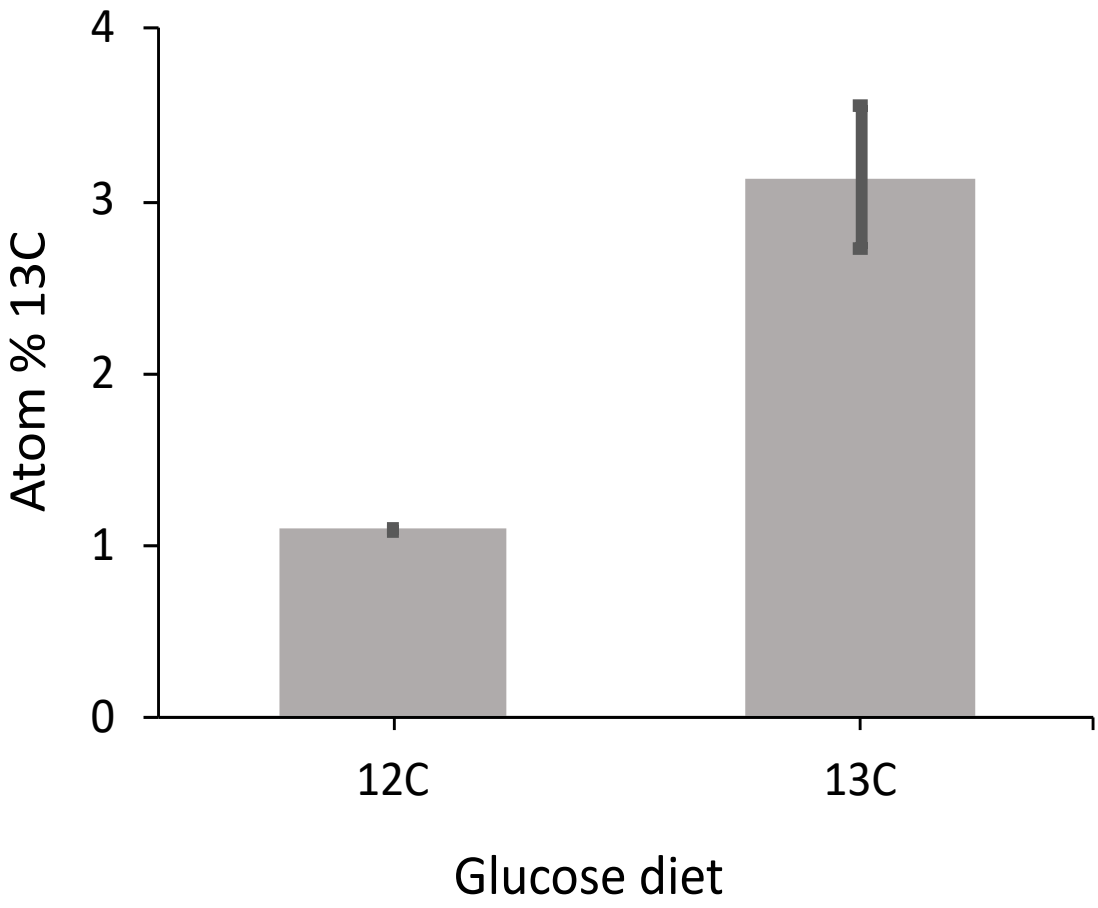

Figure S5. The atom percentage of ^{13}C in ants fed either a ^{12}C or ^{13}C labeled 20% (w/v) glucose diet for 10 days, as determined by Isotope Ratio Mass Spectrometry (IRMS) analysis.

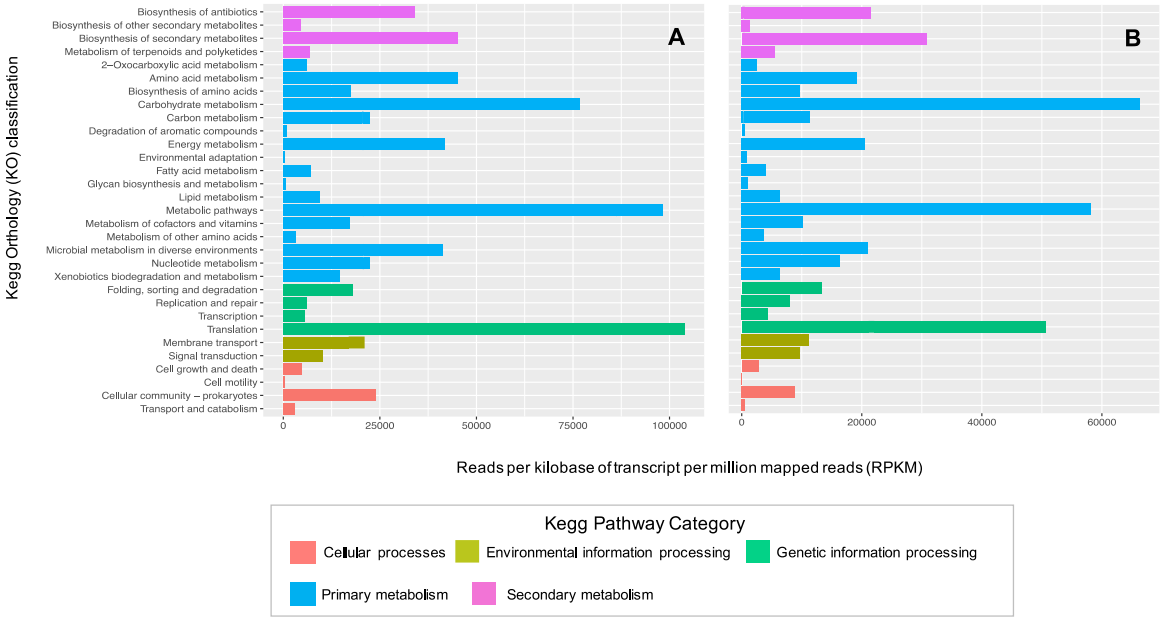

Figure S6. Expression levels (in reads per kilobase of transcript per million mapped reads, RPKM) of Kegg orthology pathway categories. (A) *Pseudonocardia octospinosus* (colony Ae088) and (B) *Pseudonocardia echinatior* (colony Ae1083) on the propleural plates of *Acromyrmex echinatior* ants. N= 1 sample of 80 pooled ants per colony.

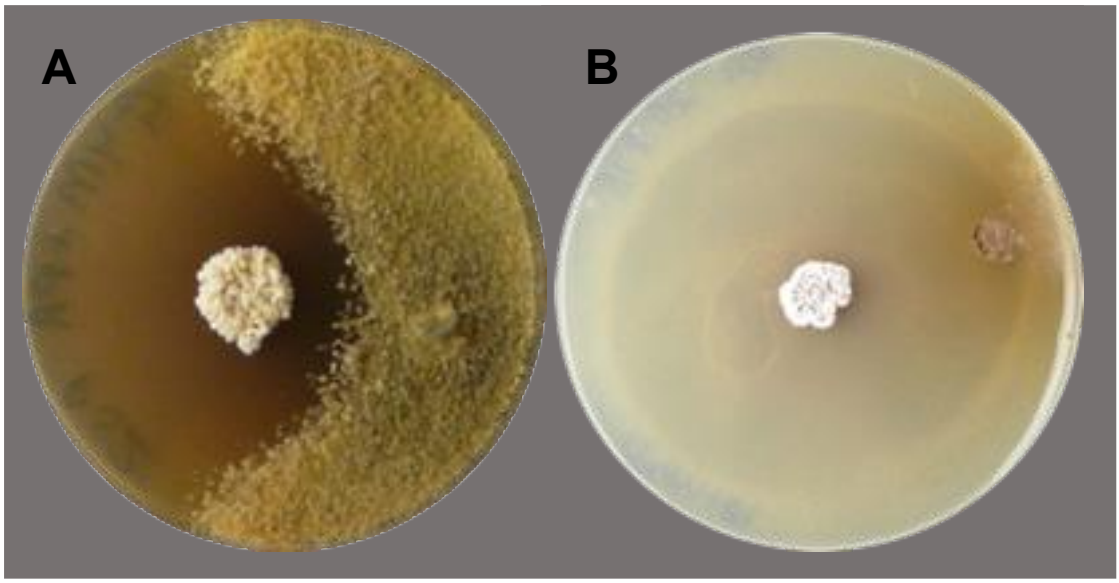

Figure S7. The bioactivity of *Pseudonocardia* isolates (**A)** *P. echinatior* PS088 and (**B)** *P. octospinosus* PS1083 against the specialized fungus-garden pathogen *Escovopsis weberi* (Table S1).

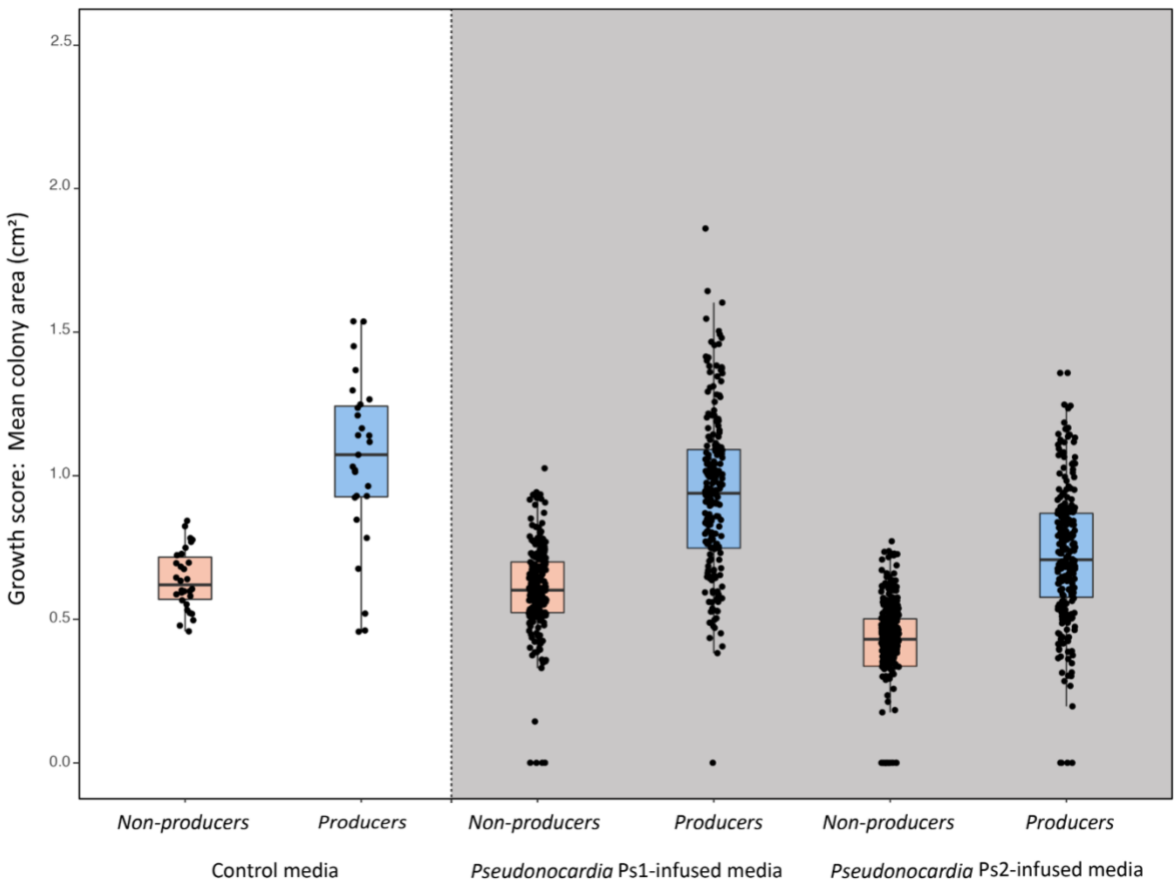

Figure S8. Individual growth-rate experiments of *Acromyrmex*-resident, non-producer strains, assessed as bacterial colony sizes after 5 days at 30 ºC, with the boxplots indicating medians ± one quartile. The white section shows growth rates on control media, and the grey section shows growth rates on the *Pseudonocardia*-infused media. Red boxes represent non-producer strains, and blue boxes represent producer strains. For analysis, a linear mixed-effects model, including *Pseudonocardia* strain (n=17) and inoculated bacterial species (n=20) as random factors, was used to test for interactions and main effects of growth media (Control vs. Ps1-infused vs. Ps2-infused) and antibiotic production (non-producers vs. *Streptomyces*). There was no significant interaction effect (χ^2 = 2.64, df = 2, p = 0.27), but both main effects were highly significant. The resident non-producers isolated from cuticular microbiomes had significantly slower growth rates on all media (χ^2 = 20.96, df = 1, p < 0.0001) including the control media without antibiotics. This suggests that they are unable to outcompete producer strains on the cuticle of *Acromyrmex* ants and raises the question why these non-producer species can persist at all. Bacterial growth was also generally slower on Ps2-infused media than on Ps1-infused media (χ^2 = 21.43, df = 1, p < 0.000 when analyzed in a balanced design without the control-media).

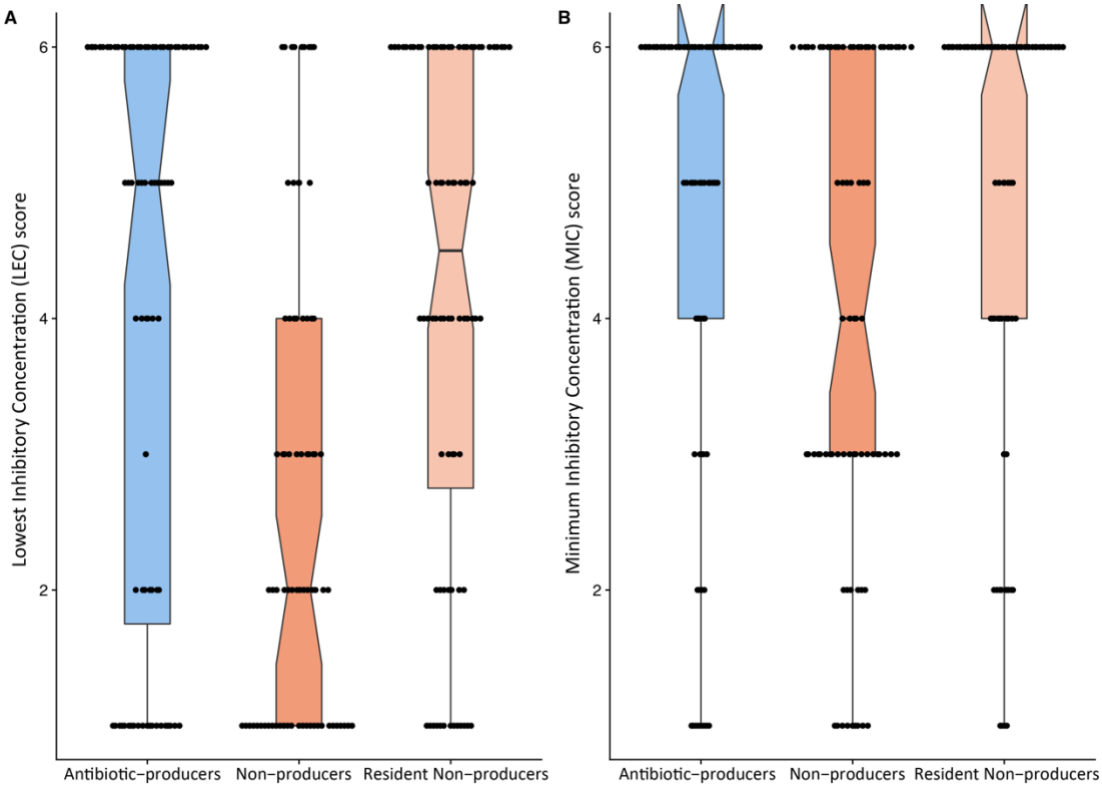

Figure S9. Antibiotic resistance profiles for producer, non-producer, and resident non-producer strains (Table S1). Boxplots indicate medians (notches) ± one quartile. For analysis, we calculated each strain's mean growth score across the eight tested antibiotics (reducing from n = 155 to n = 20). Producers showed higher levels of resistance than did non-producers for both measurements: Wilcoxon two-sided test (wilcox.test), W = 94.5, p = 0.0017 for LEC (**A**) and W = 80, p = 0.0253 for MIC (**B**), after correction for multiple testing. Producers and Resident non-producers showed no difference in resistance levels (p = 0.44 and 0.25). The 'rabbit ears' in **B** indicate that the medians are also the highest values. Data and details of the analysis are included in the code for Figure 5 (see Statistical Analyses in the Methods section).

Table S1. Details of ant colonies, bacterial strains and fungal strains, reference genomes and primers used in experiments. ***Pseudonocardia* strains that have been genome-sequenced. †*Pseudonocardia* strains that were only used in the growth-rate experiment with non-producers.

Ant colony name	Description	Origin
Ae1083	*Acromyrmex echinatior* ant colony harboring *Pseudonocardia octospinosus.*	Gamboa, Panama.
Ae088	*Acromyrmex echinatior* ant colony harboring *Pseudonocardia echinatior*.	Gamboa, Panama.
Microbial strain	**description**	**origin**
PS1083	*Pseudonocardia octospinosus* isolated from *Acromyrmex echinatior* ants in colony Ae1083.	Isolated in this study
PS088	*Pseudonocardia echinatior* isolated from *Acromyrmex echinatior* ants in the colony Ae088.	Isolated in this study
CBS 810.71	Strain of the parasitic fungus *Escovopsis weberi.*	Westerdijk Fungal Biodiversity Institute
8 *Pseudonocardia* Ps1 strains		
Ae356*	Derived from colony Ae356	Holmes *et al.* [32]
Ae263*	Derived from colony Ae263	Holmes *et al.* [32]
Ae322	Derived from colony Ae322	This Study
Ae150A*	Derived from colony Ae150A	Holmes *et al.* [32]
Ae168*	Derived from colony Ae168	Holmes *et al.* [32]
Ae707-CP-A2* (Ae707_Ps1)	Derived from colony Ae707-CP-A2	Holmes *et al.* [32]
Ae712†	Derived from colony Ae712	This Study
Ae280†	Derived from colony Ae280	This Study

11 *Pseudonocardia* Ps2 strains		
Ae406*	Derived from colony Ae406	Holmes *et al.* [32]
Ae160	Derived from colony Ae160	This Study
Ae505*	Derived from colony Ae505	Holmes *et al.* [32]
Ae717*	Derived from colony Ae717	Holmes *et al.* [32]
Ae703	Derived from colony Ae703	This Study
Ae702	Derived from colony Ae702	This Study
Ae707	Derived from colony Ae707	This Study
Ae331*	Derived from colony Ae331	Holmes *et al.* [32]
Ae706*	Derived from colony Ae706	Holmes *et al.* [32]
Ae704	Derived from colony Ae704	This Study
Ae715	Derived from colony Ae715	This Study
10 environmental antibiotic-producing strains (all *Streptomyces*)		
S1. *S. coelicolor* M1146	*Streptomyces coelicolor* M145 Δ*act* Δ*red* Δ*cpk* Δ*cda*	John Innes Centre, Norwich, NR4 7UH, UK [48]
S2. *S. lividans 66*	Soil derived *Streptomyces* species	John Innes Centre, Norwich, NR4 7UH, UK [49]
S3. *S. coelicolor* M145	Soil derived *Streptomyces*, SCP1- SCP2- Pgl+	John Innes Centre, Norwich, NR4 7UH, UK [50]
S4. *S. scabies* 87-22	Soil derived *Streptomyces* species	Bignell *et al.* [51]
S5. *S. venezuelae* NRRL B-65442	Soil derived *Streptomyces* species	USDA ARS Culture Collection. https://nrrl.ncaur.usda.gov/cgi-bin/usda Strain no. B-65442.
S6. *S.* Ae150A-B1	*Streptomyces* derived from lab workers of captive colony Ae150A	This study

S7. *S.* Ae356-S1	*Streptomyces* derived from lab workers of captive colony Ae356	This study
S8. *S. formicae* KY5	*Tetraponera penzigi* derived *Streptomyces* species	Seipke *et al.* [52], Holmes *et al* [53]
S9. *S.* S4	*Acromyrmex octospinosus* derived *Streptomyces albidoflavus* S4	Barke *et al*. [37]; Seipke *et al.*[47]
S10. *S.* S4 Δ*antA::apr*	*Streptomyces albidoflavus* S4 Δ*antA::apr*	Seipke *et al.* [54]
10 environmental non-producer strains		
St1. *Escherichia coli*	Non-pathogenic ESKAPE laboratory screening strain	ATCC® 11775™
St2. *Lysobacter antibioticus*	Non-pathogenic ESKAPE laboratory screening strain	Handelsman Lab, Small World Initiative, University of Wisconsin-Madison, USA
St3. *Bacillus subtilis*	Non-pathogenic ESKAPE laboratory screening strain	Handelsman Lab, Small World Initiative, University of Wisconsin-Madison, USA
St4. *Pseudomonas putida*	Non-pathogenic ESKAPE laboratory screening strain	Handelsman Lab, Small World Initiative, University of Wisconsin-Madison, USA
St5. *Erwinia caratova*	Non-pathogenic ESKAPE laboratory screening strain	Handelsman Lab, Small World Initiative, University of Wisconsin-Madison, USA
St6. *Enterobacter aerogenes*	Non-pathogenic ESKAPE laboratory screening strain	ATCC® 51697™
St7. *Acinetobacter baylyi*	Non-pathogenic ESKAPE laboratory screening strain	ATCC® 33305™

St8. *Staphylococcus epidermidis*	Non-pathogenic ESKAPE laboratory screening strain	ATCC® 14990™
St9. *Micrococcus luteus*	*Micrococcus luteus* (NCTC2665, "Fleming strain")	ATCC® 4698™
St10. *Serratia* KY15	*Tetraponera penzigi* derived *Serratia*	Seipke *et al.* [52]
10 *Acromyrmex*-resident non-producer strains		
Sr1. *Ochrobactrum sp*	*Acromyrmex* derived	This study
Sr2. *Erwinia* sp.	*Isolated from large A. echinatior worker ants in lab colonies*	This study
Sr3. *Acinetobacter* sp.	*Isolated from large A. echinatior worker ants in lab colonies*	This study
Sr4. *Sphingobacterium sp.*	*Isolated from large A. echinatior worker ants in lab colonies*	This study
Sr5. *Acinetobacter* sp.	*Isolated from large A. echinatior worker ants in lab colonies*	This study
Sr6. *Luteibacter sp.*	*Isolated from large A. echinatior worker ants in lab colonies*	This study
Sr7. *Flavobacterium sp.*	*Isolated from large A. echinatior worker ants in lab colonies*	This study
Sr8. *Brevundimonas sp.*	*Isolated from large A. echinatior worker ants in lab colonies*	This study
Sr9. *Acinetobacter sp.*	*Isolated from large A. echinatior worker ants in lab colonies*	This study

Sr10. *Brachybacterium sp.*	*Isolated from large A. echinatior worker ants in lab colonies*	This study
Genome	**Description**	**Accession number/ reference**
Acromyrmex echinatior	Whole genome shotgun sequencing project of the *A. echinatior* genome.	AEVX00000000; Nygaard *et al.* [55]
Ae707	Whole genome shotgun sequencing of a wild-type isolate of *Pseudonocardia octospinosus*, isolated from the cuticle of a large worker.	MCIR00000000; Holmes *et al.* [32]
Ae706	Whole genome shotgun sequencing of a wild-type isolate of *Pseudonocardia echinatior*, isolated from the cuticle of a large worker.	MCIQ00000000; Holmes *et al.* [32]
Primer	**Sequence**	**Reference**
341F	5'-CCTACGGG AGGCAGCAG-3'	Amplifies the V3 region of the 16S rRNA gene [56]
518R	5'- ATTACCGCGGCTGCTGG -3'	

Table S2. The total number of RNA-sequencing reads (and percentage of total reads in brackets) originating from propleural plate samples taken from the ant colonies Ae1083 or Ae088, respectively, that successfully aligned to the *A. echinatior* genome (Table S1) and to the genomes of the *Pseudonocardia* species associated with the ant colony of origin (*P. octospinosus* or *P. echinatior*, respectively).

Sample	**Source**	**Alignment**		
		***A. echinatior* genome**	***P. octospinosus* genome Ae707**	***P. echinatior* genome Ae706**
Ae1083	80 pooled sets of propleural plates from large workers	8,548,640 (78.7 %)	103,820 (1.0 %)	-
Ae088	80 pooled sets of propleural plates from large workers	7,058,678 (73.5 %)	-	189,989 (2.0 %)

Table S3. Secondary metabolite BGCs in the *Pseudonocardia* mutualist genomes (table adapted from Holmes *et al.* [32]) and their associated expression values (in reads per kilobase of transcript per million mapped reads, RPKM) in RNA-sequencing experiments. Yellow rows are BGCs shared between strains. Green and blue represent BGCs that are unique to *P. octospinosus* and *P. echinatior*, respectively.

Cluster number		**Classification**	**Cluster code**	**RPKM expression values**	
P. octospinosus	***P. echinatior***			***P. octospinosus***	***P. echinatior***
1	7	Oligosaccharide	A	57.05	45.47
5	5	Terpene	B	81.19	37.58
7	4	Nystatin	C	1.76	24.28
8	2	Terpene	D	341.82	424.23
11	9	Bacteriocin	E	118.95	80.24
14	8	Ectoine	F	453.11	192.08
2	-	Other	G	34.34	-
3	-	Other	H	110.18	-
4	-	NRPS	I	10.97	-
6	-	Bacteriocin	J	111.07	-
9	-	NRPS	K	41.92	-
12	-	Other	L	52.55	-
13	-	NRPS	M	25.64	-
-	1	Other	N	-	16.75
-	3	T1PKS-NRPS	O	-	16.87
-	6	Bacteriocin	P	-	91.71
-	10	Terpene	Q	-	23.75
-	11	Bacteriocin	R	-	30.50

Table S4. Media recipes and antibiotics used in this study.

Medium Name	Component	g L^{-1} dH_2O	
Soya Flour Mannitol (SFM) Agar	Soy flour	20	
	Mannitol	20	
	Agar	20	
Potato Glucose Agar (PGA)	PGA (Sigma Aldrich)	39	
Glucose, Yeast, Malt (GYM) Agar	Glucose	4	
	Yeast extract	4	
	Malt extract	10	
	CaCO3	2	
	Agar	15	
Lennox Broth (LB)	Tryptone	10	
	NaCl	10	
	Yeast extract	5	
Antibiotic	**Concentrations Used**	**Target**	**Compound Type**
Chloramphenicol	0, 2.5, 5, 10, 25, 50 µg/ml	Translation inhibitor	Synthetic
Rifampicin	0, 0.5, 1, 2, 5, 10 µg/ml	Translation inhibitor	Polyketide
Streptomycin	0, 5, 10, 20, 50, 100 µg/ml	Translation inhibitor	Aminoglycoside
Vancomycin	0, 1, 2, 4, 10, 20 µg/ml	Cell wall synthesis inhibitor	Glycopeptide

Phosphomycin	0, 5, 10, 20, 50, 100 µg/ml	Cell wall synthesis inhibitor	Small molecule
Nalidixic Acid	0, 2.5, 5, 10, 25, 50 µg/ml	DNA gyrase inhibitor	Synthetic quinolone
Apramycin	0, 5, 10, 20, 50, 100 µg/ml	Translation inhibitor	Aminoglycoside
Ampicillin	0, 10, 20, 40, 100, 200 µg/ml	Cell wall synthesis inhibitor	ß lactam